2011

Evolution of the Northwestern Margin of the Basin and Range: The Geology and Extensional History of the Warner Range and Environs, Northeastern California

Anne E. Egger
Central Washington University, annegger@geology.cwu.edu

Elizabeth L. Miller
Stanford University

Recommended Citation

Egger, A. & Miller, E.L. (2011). Evolution of the northwestern margin of the Basin and Range: The geology and extensional history of the Warner Range and environs, northeastern California. *Geosphere 7*(3), 756-773. DOI: 10.1130/GES00620.1

Evolution of the northwestern margin of the Basin and Range: The geology and extensional history of the Warner Range and environs, northeastern California

Anne E. Egger* and Elizabeth L. Miller
Department of Geological and Environmental Sciences, Stanford University, 450 Serra Mall, Building 320, Stanford, California 94305-2115, USA

ABSTRACT

Along the northwestern margin of the Basin and Range province, mid-Miocene to Pliocene volcanic rocks cover and obscure much of the earlier history of the region. In northeastern California, however, slip on the Surprise Valley fault has resulted in the uplift of the Warner Range, exposing >4 km of volcaniclastic and volcanic rocks as old as late Eocene. New geologic mapping, combined with geochemistry and geochronology of rocks in the Warner Range and surrounding region, documents a history of volcanism and extension from the Eocene to the present that provides insight into the evolution of this margin. Our work reveals that subduction-related arc volcanism began ca. 40 Ma and continued into the mid-Miocene, despite the nearby impingement of the Yellowstone hotspot and eruptions of flood basalts. Extensional normal faulting began in the mid- to late Miocene in relative isolation from other Basin and Range normal faults. Later Miocene and Pliocene volcanic rocks flowed into low-lying areas produced by mid-Miocene extension. These younger basalts are cut by normal faults, requiring a second episode of extension that began after 3 Ma. Our cross-section reconstructions indicate that 12%–15% extension has been accommodated across the Warner Range region, primarily along the Surprise Valley fault, which has accommodated 8 km of dip-slip motion. A similarly protracted or two-part history of extension has been observed elsewhere in the western Basin and Range. While relatively little extension has been accommodated in the Warner Range region, it continues to the present day. Thus, the Surprise Valley fault appears to have persisted as the westernmost boundary of Basin and Range extension since the mid-Miocene.

INTRODUCTION

Modern deformation and seismic activity across the actively extending Basin and Range province of the western United States is concentrated along its borders, where it is bounded by the unextended Sierra Nevada and Colorado Plateau, respectively (Fig. 1). Geodetic surveys have shown that the western margin of the province also accommodates 15%–25% of Pacific-North American plate motion, primarily within the Walker Lane, a 100–150-km-wide zone of distributed dextral shear (e.g., Bennett et al., 2003; Thatcher et al., 1999) (Fig. 1), highlighting the importance of the western margin of the Basin and Range to our overall understanding of plate boundary processes and deformation in western North America. A significant amount of recent work has focused on the structural evolution of the western margin of the province along the eastern side of the Sierra Nevada and the relationship between extensional and strike-slip faulting (e.g., Cashman et al., 2009; Henry et al., 2007; Oldow, 2003; Surpless et al., 2002; Trexler et al., 2000). In contrast, there have been few detailed investigations of the geologic and structural history of the northern continuation of the western margin of the Basin and Range—the portion of the boundary that lies north of the Sierra Nevada and east of the Cascades (dashed line, Fig. 1).

Several features set the northwestern margin of the Basin and Range apart from its better-studied southern counterpart. First, its tectonic setting differs in that it lies north of the Mendocino Triple Junction and thus inboard of a modern subduction zone rather than the San Andreas strike-slip plate boundary (Fig. 1). South of the triple junction, the Walker Lane lies within the Basin and Range and WNW-ESE-directed extension occurs both to the east and west of the zone of dextral shear (Cashman et al., 2009; Surpless, 2008). North of the triple junction, dextral strike-slip faulting interpreted as northward propagation of the Walker Lane dies out to the west of significant extension in the Basin and Range (Fig. 1) (Faulds et al., 2005; Unruh et al., 2003). Second, the amount of extension that has occurred in the northwestern portion of the Basin and Range is significantly less than that farther south in the province. Here, normal faults associated with Miocene and younger extension decrease in offset and die out northwards, transitioning to the relatively unextended High Lava Plains of southern Oregon (Fig. 1) (Jordan et al., 2004; Lerch et al., 2008; Scarberry et al., 2010). In comparison, the western margin of the Basin and Range further south has undergone high-magnitude extension (>100%) such as in the Singatse-Wassuk region (Proffett and Dilles, 1984; Surpless et al., 2002) (Fig. 1). As a result of relatively little extension, pre-Tertiary basement is rarely exposed along the northwestern margin.

Finally, the northwestern margin of the Basin and Range has experienced a different Tertiary magmatic history than much of the rest of the province. Andesitic magmatism related to subduction was reestablished in the region as early as ca. 40 Ma (Colgan et al., 2011), as opposed to only ca. 16 Ma further south (e.g., Busby et al., 2008), but this earlier evolution of the region is largely buried by voluminous mid-Miocene and younger volcanic rocks. Yellowstone hotspot volcanism began in the region ca. 16 Ma with a massive outpouring of flood basalts (the Steens and Columbia River basalts) (e.g., Hooper et al.,

*annegger@stanford.edu. Note: As of 1 September 2011, corresponding author's contact information is Department of Geological Sciences, Central Washington University, 400 University Way, Ellensburg, Washington 98926, USA; annegger@geology.cwu.edu.

Geosphere; June 2011; v. 7; no. 3; p. 756–773; doi:10.1130/GES00620.1; 7 figures; 1 table; 1 plate; 1 supplemental database file.

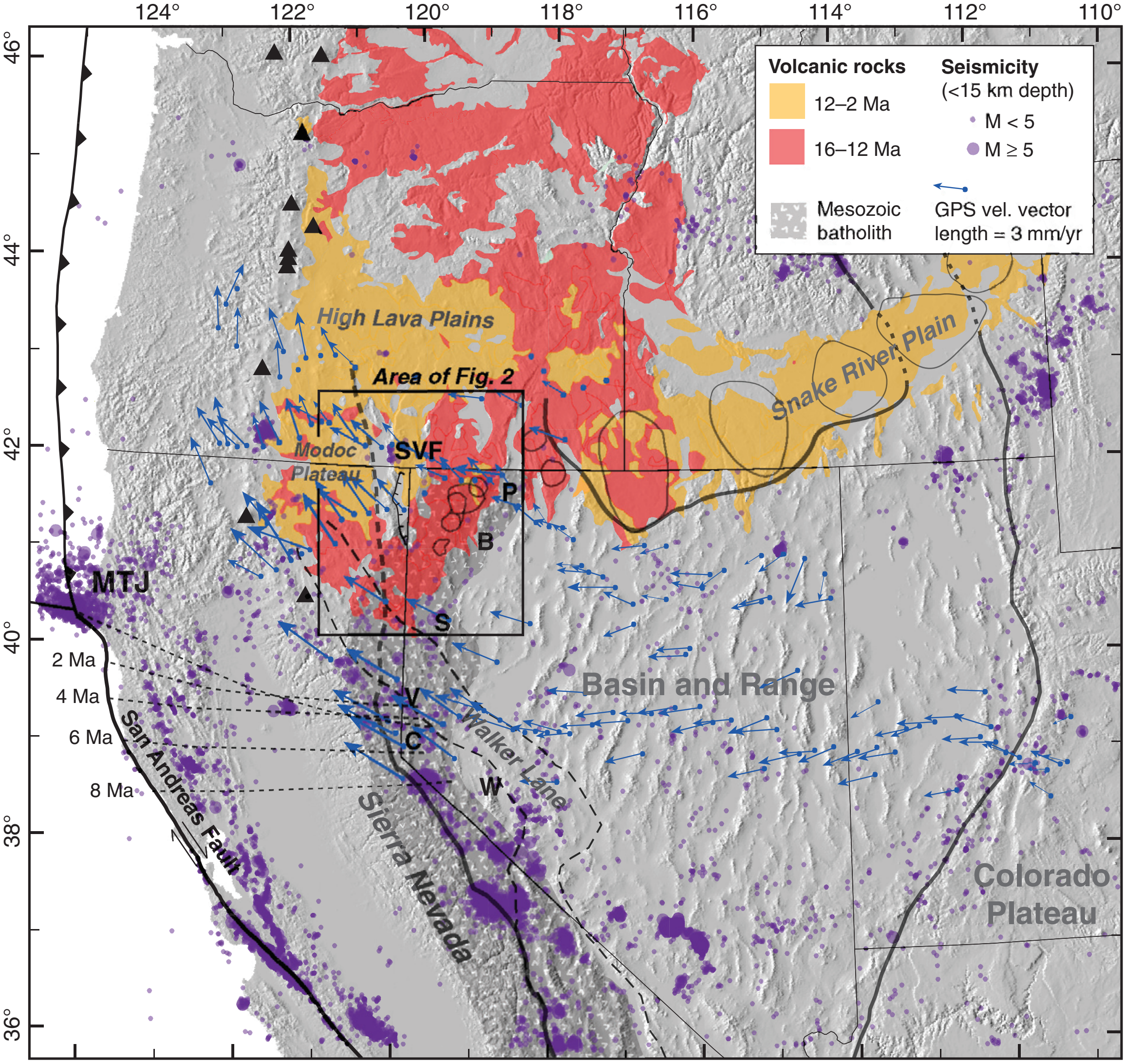

Figure 1. Selected tectonic features in the western U.S. and main region of Neogene volcanic rocks along the northern and western boundary of the Basin and Range province from Reed et al. (2005). Thick gray lines show approximate boundary of the Basin and Range province. Black triangles—active volcanoes of the Cascades. Inferred Yellowstone hotspot calderas outlined with thin gray lines after Pierce and Morgan (1992) in the Snake River Plain and Coble and Mahood (2008) in northwest Nevada. Main region underlain by Mesozoic batholithic rocks after Van Buer et al. (2009). Northern Walker Lane extent after Faulds et al. (2005); southern after Wesnousky (2005). Short dashed lines—location of Mendocino edge of subducting Juan de Fuca slab over the last 8 Ma (Atwater and Stock, 1998). GPS velocity vectors from Hammond and Thatcher (2004, 2005). Earthquake data from the Northern California Earthquake Catalog and Advanced National Seismic System (ANSS) Worldwide Earthquake Catalog. Localities referred to in text: B—Black Rock Range; C—Carson Range; P—Pine Forest Range; S—Shawave Range; SVF— Surprise Valley fault; V—Verdi-Boca Basin; W—Wassuk Range.

2002) and was followed closely by the development of rhyolitic calderas, now exposed on the Sheldon Plateau (Figs. 1 and 2) (Coble and Mahood, 2008; Greene, 1984). A younger episode of widespread volcanism occurred in the Modoc Plateau region (Fig. 1) and lasted from ca. 8 to 3 Ma; this later episode is dominated by smaller volume, more mafic eruptions of distinctive low-potassium, high-alumina olivine tholeiites that filled low-lying topography and remain mostly undissected (Carmichael et al., 2006; McKee et al., 1983).

Within this region that is largely obscured by young volcanic rocks, the Warner Range in northeastern California provides a unique opportunity to learn more about both the pre-Miocene tectonic and magmatic history of the northwestern Basin and Range and the evolution of the margin since extension began. Uplifted by motion along the Surprise Valley fault, the Warner Range exposes a thick section of volcanic, volcaniclastic, and sedimentary rocks that record a semicontinuous history of magmatism and sedimentation dating back to the late Eocene. The mountain range thus provides a critical window into the earlier magmatic and structural evolution of the region. The Surprise

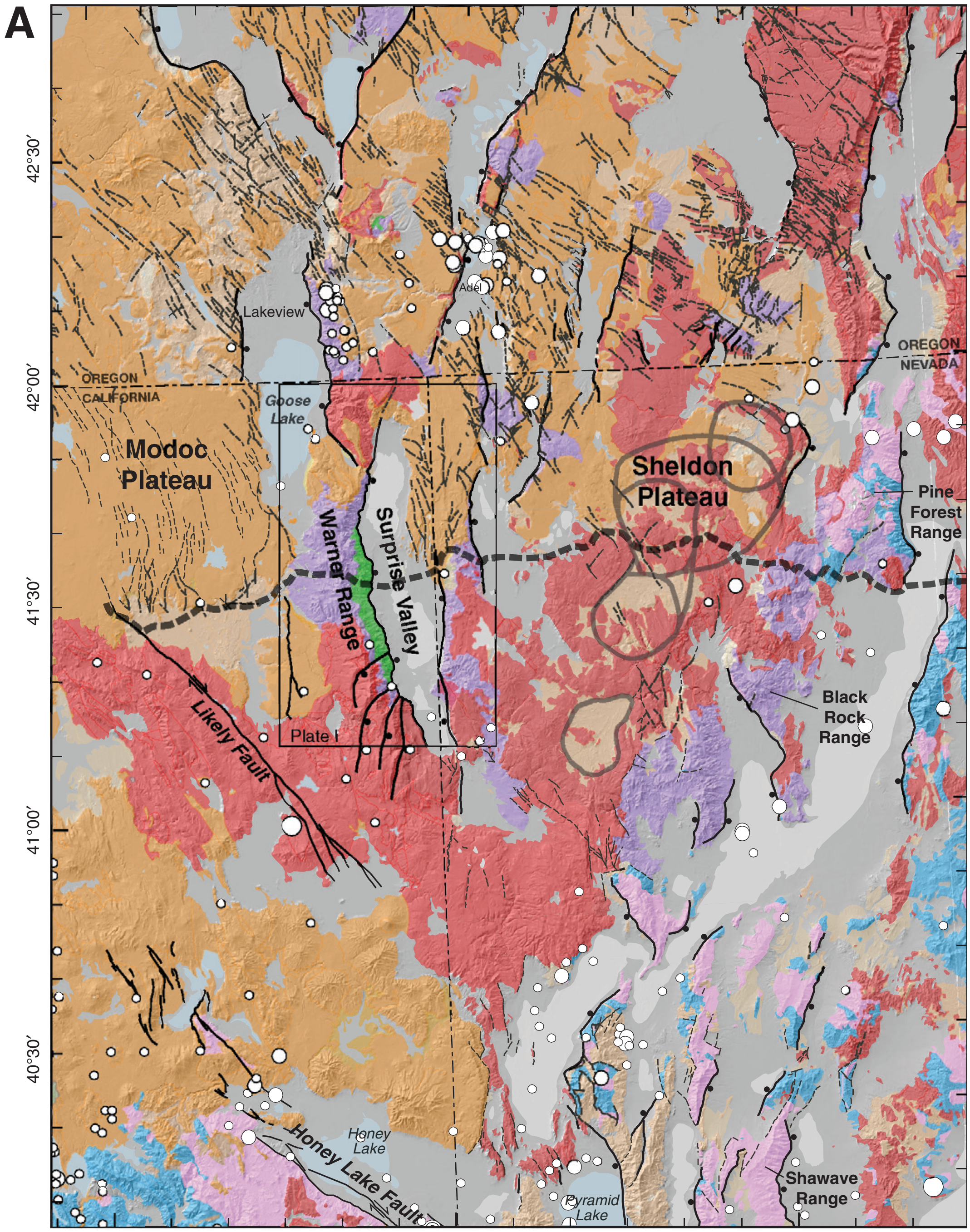

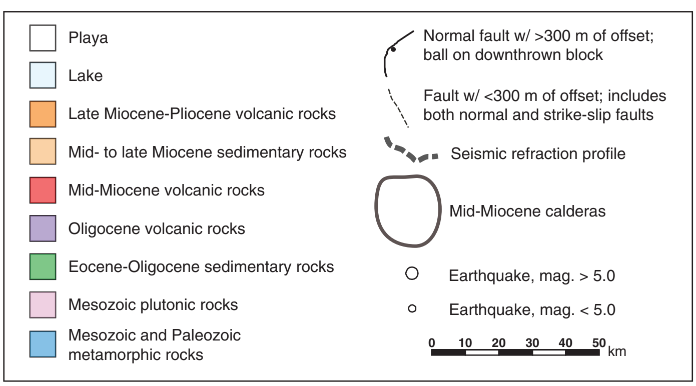

Figure 2 (*on this and following page*). (A) Simplified geologic map, from state geologic maps, and index to Plate 1. Outlines of mid-Miocene calderas from Coble and Mahood (2008). Dashed line shows location of seismic refraction profile (Lerch et al., 2007).

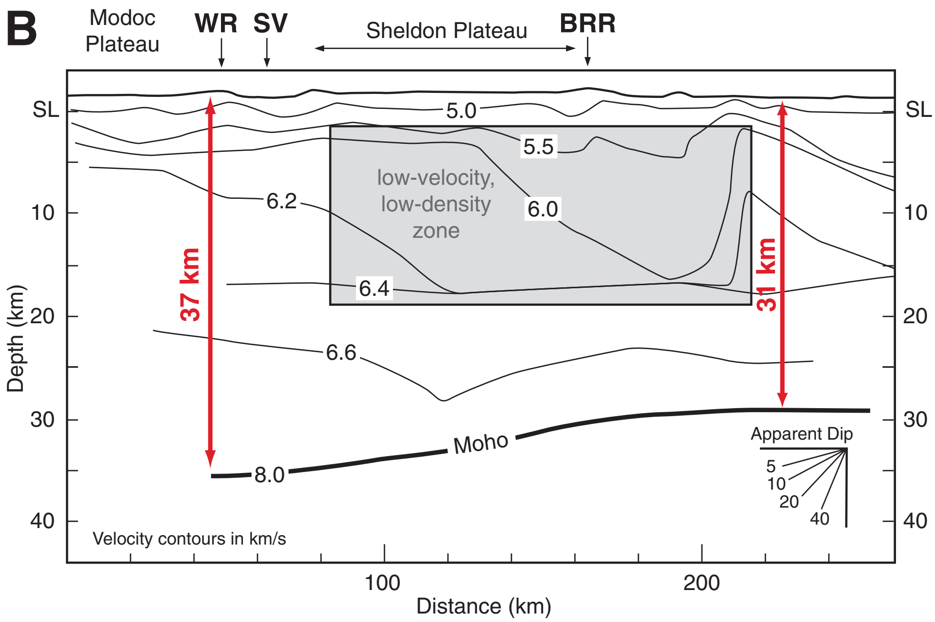

Figure 2 (*continued*). (B) Crustal velocity profile, modified from Lerch et al. (2007). WR—Warner Range, SV—Surprise Valley, BRR—Black Rock Range. Box encloses low-velocity zone interpreted as the northward continuation of the Sierra Nevada batholith in the subsurface.

Valley fault (SVF), ~85 km long with ~8 km of total dip-slip motion, is similar in extent and offset to other large Basin and Range faults, but it lies 80–100 km from those other faults in the direction parallel to extension (Fig. 2), much further than typical Basin and Range fault spacing of 20–30 km (Stewart, 1971). As a result of its relative isolation, the slip history of the SVF can thus be assumed to describe the evolution of extension along this margin from its inception to the present day. The geologic mapping and cross sections presented here provide new details about the geology, volcanic history, and structural evolution of the Warner Range and surrounding region that elucidate the history of the less studied and more enigmatic northwestern margin of the Basin and Range and lend insight into long-term plate boundary processes.

PREVIOUS WORK

In comparison to most of the western margin of the Basin and Range, the region encompassing the Warner Range has been sparsely mapped and studied. Russell (1928) pursued reconnaissance mapping in the Warner Mountains because he believed that, unlike much of the rest of the "Basin ranges," no previous episode of folding had disturbed the layers of sedimentary and volcanic rocks, and the faulting event that produced the modern topography could be studied in isolation. Numerous subsequent investigators focused on a single aspect of the stratigraphy of the range, primarily the well-preserved Eocene and Oligocene flora in the sedimentary sequence at the base of the range (Axelrod, 1966; MacGinitie, 1941; Myers, 1998, 2003, 2006).

Martz (1970) mapped the central portion of the range, adding detail to Russell's earlier reconnaissance mapping, particularly in the lower sedimentary sequence (Fig. 3). Geological mapping in the southern portion of the Warner Range was undertaken for the purposes of assessing potential mineral resources prior to the designation of the South Warner Wilderness Area (Fig. 3) (Duffield and Weldin, 1976). As part of that study, Duffield and McKee (1986) dated several volcanic units exposed in the range, establishing the Oligocene age of the sedimentary section and mid-Miocene age of rocks at the crest of the range (Table 1). Carmichael et al. (2006) added significantly to the geochronological and geochemical database for the region in their study of the nature and extent of late Miocene and Pliocene lava flows, previously described farther west on the Devil's Garden Plateau by McKee et al. (1983).

Hedel (1980, 1981, 1984) mapped Quaternary fault scarps in the Surprise Valley; these were more closely studied and verified in the field and with photogeologic methods by Bryant (1990). A seismic reflection profile was collected across the Surprise Valley (Lerch et al., 2010) and, together with potential field data, numerous intrabasin faults were identified (Egger et al., 2010). A trench was dug across the Surprise Valley fault for paleoseismic studies to determine earthquake recurrence intervals in this region (Personius et al., 2009). Geothermal exploration continues in the region today, resulting in the drilling of a core north of Lake City (Fig. 3) (Benoit et al., 2005; Egger et al., 2009).

On a regional scale, geophysical studies have shown that the crust beneath the northwestern margin of the Basin and Range thins homogeneously from ~37 km thick beneath the Modoc Plateau (and the Warner Range) to ~31 km beneath northwestern Nevada (Fig. 2B) (Lerch et al., 2007). Potential field modeling shows that the velocity and density of upper crustal units also changes across this transition: the Warner Range lies west of a 15-km-thick low-velocity, low-density ($V_p \approx 6.0$ km/s), and low V_p/V_s zone in the upper crust (Fig. 2B) interpreted as the northward continuation of the Sierra Nevada batholith (Fig. 1) (Gashawbeza et al., 2008; Lerch et al., 2007; Van Buer et al., 2009).

NEW GEOLOGIC MAPPING

The primary result of this study is a new 1:100,000-scale geologic map and reconstructed cross sections of the Warner Range and surrounding region, included here as Plate 1 and as an ArcGIS database (see supplemental database file[1]). In order to prepare the map and cross sections, we conducted detailed geologic mapping in the Warner Range north and west of the South Warner Wilderness and south of Fandango Valley, in the hills north of the Hays Canyon Range, and along the western range front of the Hays Canyon Range, while reconnaissance mapping was conducted in the surrounding region (see Figure 3 for locations). Using digital orthophotoquads and field-checking key locations, we mapped Quaternary deposits within the valley.

We also compiled and digitized mapping from the original field maps that were included in the 1:48,000 scale map of Duffield and Weldin (1976): by overlaying orthophotoquads on digital elevation models, we were able to add substantial detail and revised significant portions of the previously mapped South Warner Wilderness. Quaternary fault scarp mapping by Hedel (1981) and Bryant (1990) was digitized

[1]Supplemental Database File. ArcGIS geodatabase from which Plate 1 was made. ArcGIS software is required to open the database. If you are viewing the PDF of this paper or reading it offline, please visit http://dx.doi.org/10.1130/GES00620.S2 or the full-text article on www.gsapubs.org to view the supplemental database file.

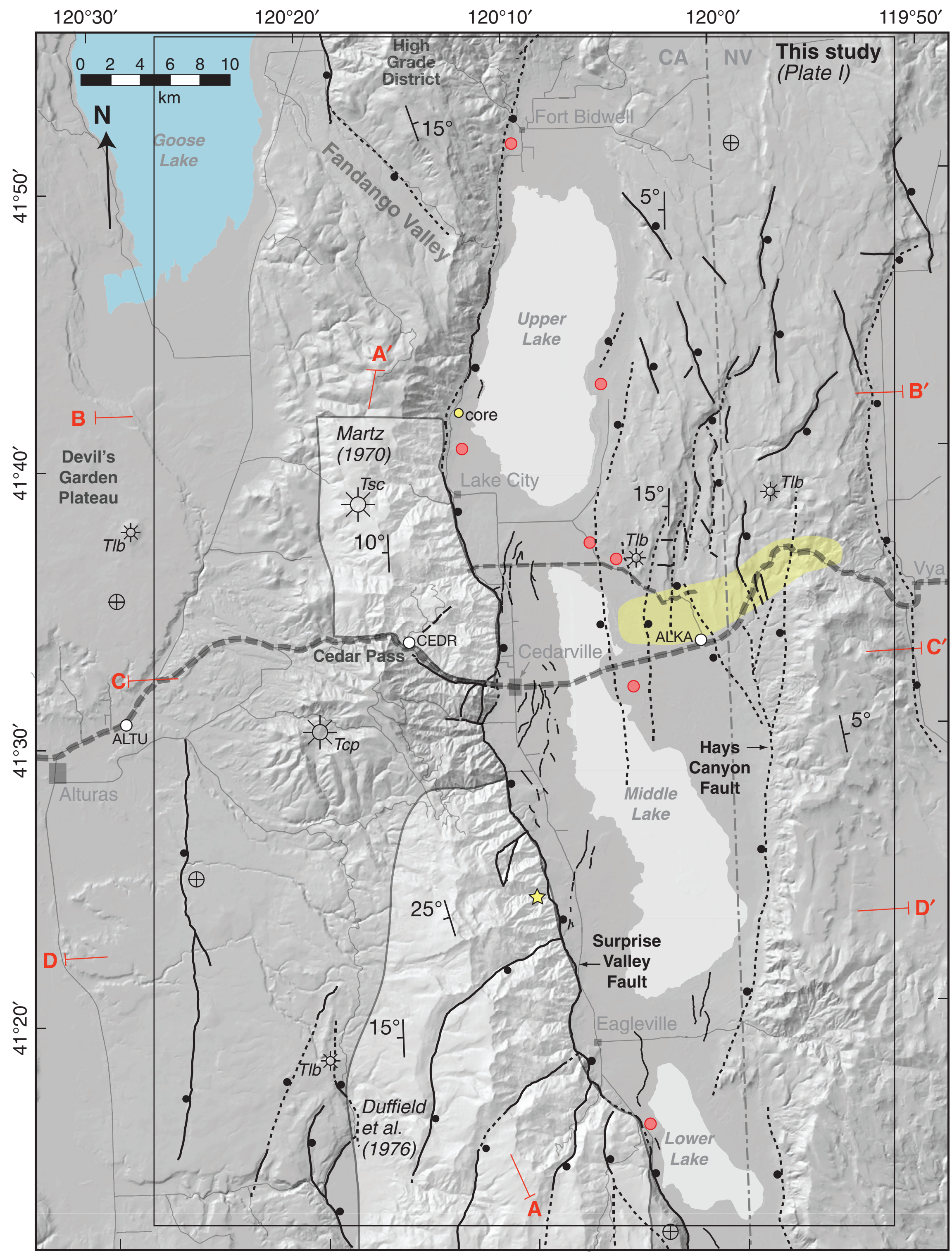

Figure 3. Cenozoic fault map (ball on downthrown block) and index of previous work in the Warner Range region. Black stars are approximate volcanic vent locations and their map unit labels as described in text and Plate 1. Thin dashed gray line is the seismic reflection line (Lerch et al., 2010) along which seismic velocity and potential field models were constructed (Egger et al., 2010). Thicker dashed gray line is the location of the seismic refraction profile also shown in Figure 2 (Lerch et al., 2007). Red lines—cross-section lines (Plate 1, Fig. 6). Yellow star—thermochronology sample studied by Colgan et al. (2008). Red circles—hot spring locations. White circles—GPS stations (Hammond and Thatcher, 2007). Yellow shaded region is the accommodation zone described in the text. Cross-section A–A′ shown in Figure 4; others shown in Figure 6.

TABLE 1. GEOCHRONOLOGY OF WARNER RANGE REGION VOLCANIC ROCKS

Sample	Longitude*	Latitude*	Map Unit	Rock Type	Method	Mineral	Age (±1σ)†	Data Source§
Eocene volcanic rocks								
F0457	–120.19123	41.57976	Tmrv	Andesite lava	K-Ar	feldspar	40.8 ± 3.0#	Axelrod (1966)
Oligocene sedimentary sequence								
D63B	–120.15444	41.38333	Tsu	Andesitic ash	K-Ar	hornblende	33.9 ± 2.7	Duffield & McKee (1986)
unreported	Granger Canyon		Tsu	Volcanic sandstone	^{40}Ar/^{39}Ar	unknown	31.56 ± 0.42	Myers (1998)
D113B	–120.16833	41.42083	Tsu	Andesitic ash	K-Ar	hornblende	31.1 ± 1.3	Duffield & McKee (1986)
unreported	Badger's Nose		Tsu	Andesitic ash	^{40}Ar/^{39}Ar	unknown	30.19 ± 0.48	Myers (1998)
699_15A	–120.22167	41.50000	Tdc (?)	Andesitic ash	K-Ar	hornblende	28.8 ± 1.1	Duffield & McKee (1986)
Lake City basalts								
JC08-WR405	–120.23168	41.60900	Tovl	Basalt	^{40}Ar/^{39}Ar	groundmass	27.83 ± 0.21	Colgan et al. (2011)
WR07AE40	–120.25011	41.70415	Tovl	Basalt	^{40}Ar/^{39}Ar	plagioclase	27.79 ± 0.61	Colgan et al. (2011)
AE05WR03	–120.22406	41.57833	Tovl	Basalt (basal flow)	^{40}Ar/^{39}Ar	plagioclase	27.17 ± 0.33	Colgan et al. (2011)
07-C-6	–120.24034	41.60912	Tovl	Olivine basalt flow	^{40}Ar/^{39}Ar	plagioclase	27.14 ± 0.08	Colgan et al. (2011)
Cedar Pass complex								
SV70a	–120.2612	41.4920	Tcp	Basaltic andesite	^{40}Ar/^{39}Ar	groundmass	30.02 ± 0.52**	Carmichael et al. (2006)
966_15	–120.2717	41.5883	Tcp	Andesite	K-Ar	hornblende	28.7 ± 1.1	Duffield & McKee (1986)
SV96	–120.2583	41.5090	Tcp	Basaltic andesite	^{40}Ar/^{39}Ar	groundmass	27.07 ± 0.22**	Carmichael et al. (2006)
H08-57	–120.24623	41.60567	Tcp	Ashflow tuff	^{40}Ar/^{39}Ar	sanidine	26.642 ± 0.077	Colgan et al. (2011)
433	–120.3222	41.5083	Tcp	Andesite	K-Ar	hornblende	26.6 ± 1.1	Duffield & McKee (1986)
WR07-AE49	–120.22595	41.48698	Tcp	Basalt plug	^{40}Ar/^{39}Ar	plagioclase	26.86 ± 0.08	Colgan et al. (2011)
07-C-19	–120.27277	41.58808	Tcp	Andesite lava	^{40}Ar/^{39}Ar	plagioclase	26.736 ± 0.045	Colgan et al. (2011)
D27B	–120.2164	41.4389	Tcp	Ashflow tuff	K-Ar	biotite	26.3 ± 1.0	Duffield & McKee (1986)
SV163	–119.89567	41.60400	Tcp††	Dacite ashflow	^{40}Ar/^{39}Ar	dacite glass	26.26 ± 0.13	Carmichael et al. (2006)
JC07-WR303	–120.26150	41.61350	Tcp	Rhyolite ashflow tuff	^{40}Ar/^{39}Ar	sanidine	26.35 ± 0.11	Colgan et al. (2011)
JC08-WR412	–120.21734	41.43877	Tcp	Ashflow tuff	^{40}Ar/^{39}Ar	sanidine	25.765 ± 0.061	Colgan et al. (2011)
JC08-WR411	–120.21417	41.44050	Tcp	Ashflow tuff	^{40}Ar/^{39}Ar	sanidine	25.526 ± 0.058	Colgan et al. (2011)
Later Oligocene volcanic rocks								
SV130	–119.89133	41.32767	Thv	Basaltic andesite	^{40}Ar/^{39}Ar	groundmass	24.55 ± 0.16	Carmichael et al. (2006)
07-C-10	–120.21695	41.43917	Tbm	Andesite lava	^{40}Ar/^{39}Ar	groundmass	24.47 ± 0.34	Colgan et al. (2011)
SV25	–119.97900	41.35317	Thv	Basaltic andesite	^{40}Ar/^{39}Ar	groundmass	23.91 ± 0.13	Carmichael et al. (2006)
Early Miocene volcanic rocks								
JC08-WR410	–120.22570	41.43801	Trt	Volcanic sandstone	^{40}Ar/^{39}Ar	sanidine	19.22 ± 0.27	Colgan et al. (2011)
1011	–120.2433	41.4606	Trt	Ashflow tuff	K-Ar	biotite	17.3 ± 0.6	Duffield & McKee (1986)
Middle Miocene volcanic rocks								
BT1	–120.2644	41.2053	Tmvu	Rhyolite	K-Ar	biotite	16.0 ± 0.5	Duffield & McKee (1986)
R54B	–120.1106	41.2383	Tmvu	Rhyolite	K-Ar	biotite	15.9 ± 0.5	Duffield & McKee (1986)
D302B	–120.1578	41.2811	Tmb	Basalt	K-Ar	whole-rock	15.8 ± 0.5	Duffield & McKee (1986)
D144B	–120.1506	41.2861	Tmb	Basalt	K-Ar	whole-rock	15.7 ± 0.5	Duffield & McKee (1986)
D474B	–120.1822	41.2117	Tmb	Basalt	K-Ar	whole-rock	15.7 ± 0.4	Duffield & McKee (1986)
SV19	–119.9335	41.2755	Tmb	Basalt (Hays Mntn)	^{40}Ar/^{39}Ar	groundmass	15.53 ± 0.11	Carmichael et al. (2006)
R38B	–120.0983	41.2433	Tmvu	Rhyolite	K-Ar	biotite	15.5 ± 0.5	Duffield & McKee (1986)
SV49	–119.9685	41.3223	Tmb	Basalt (Hays Mntn)	^{40}Ar/^{39}Ar	groundmass	15.44 ± 0.17	Carmichael et al. (2006)

(*continued*)

and is included in Plate 1. We remapped and improved upon the region previously mapped by Martz (1970) with better topographic control, and better regional context provided by geochemistry and geochronology. We also digitized sample locations from McKee et al. (1983), correcting a few errors in latitude and longitude measurements. To aid in cross-section reconstructions, we compiled data from exploratory drill holes and well logs in Surprise Valley. We also conducted numerous geochemical and geochronological analyses on rocks from this region; sample locations and values are shown in Plate 1 but the data are presented elsewhere (Colgan et al., 2011). The following two sections of this paper describe the new and compiled data: the "Geologic Units" section details the distribution, composition, and age of rock units, and the "Faults and Extension" section details the structural setting and magnitude of extension calculated here.

GEOLOGIC UNITS EXPOSED IN THE WARNER RANGE AND SURROUNDING REGION

An ~4.5-km-thick, west-dipping sequence of Eocene to upper Miocene sedimentary and volcanic rocks is exposed in the Warner Range. In his reconnaissance mapping, Russell (1928) noted that "the volcanic rocks of this region are for the most part extensive sheets lying concordantly, one above the other, bent or broken only in relation to comparatively recent Basin Range faulting." In contrast to Russell's description and that of others (e.g., Duffield and Weldin, 1976) that suggest units are conformable and laterally continuous throughout the range, our geologic mapping reveals that units are not uniformly distributed and that unit thicknesses change rapidly and dramatically along strike (Fig. 4) with multiple unconformities within the section. The unit descriptions, map relations, and geologic history we detail in this section refer extensively to Plate 1, the geologic map, and Figure 4, a series of stratigraphic columns and a N-S cross section along the length of the range.

Late Eocene–Oligocene (ca. 40–27.5 Ma) Volcaniclastic Sedimentary Rocks

The oldest rocks exposed in the Warner Range consist of deeply weathered andesitic breccias, lahars, and debris flows with minor pyroxene- and hornblende-andesite lava flows (Fig. 4). This unit, called the McCulley Ranch Formation (Tmrv) by Martz (1970), is only exposed in the central portion of the range near Cedarville (Plate 1). Axelrod (1966) reported a K-Ar age on feldspar from a flow near the top of this unit that yielded an age of 40.8 ± 3.0 Ma (corrected age). This unit may correlate with a similar andesitic sequence exposed ~90 km to the north at Drake Peak (Fig. 2), dated at 40.2 ±

TABLE 1. GEOCHRONOLOGY OF WARNER RANGE REGION VOLCANIC ROCKS (*continued*)

Sample	Longitude*	Latitude*	Map Unit	Rock Type	Method	Mineral	Age (±1σ)†	Data Source§
Middle Miocene volcanic rocks (*continued*)								
SV126	–120.0645	41.1997	Tmvu	Basalt	$^{40}Ar/^{39}Ar$	groundmass	15.36 ± 0.08	Carmichael et al. (2006)
SV153	–119.8990	41.6062	Tmb	Basalt (Hays Mntn)	$^{40}Ar/^{39}Ar$	groundmass	15.15 ± 0.55	Carmichael et al. (2006)
SV142	–120.3415	41.3795	Tmba	Basalt	$^{40}Ar/^{39}Ar$	groundmass	14.57 ± 0.08	Carmichael et al. (2006)
D398B	–120.2939	41.2817	Tmvu	Rhyolite	K-Ar	biotite	14.5 ± 0.4	Duffield & McKee (1986)
D418B	–120.2150	41.2633	Tmba	Basalt	K-Ar	whole-rock	14.1 ± 0.4	Duffield & McKee (1986)
D235B	–120.1933	41.3111	Tmba	Basalt	K-Ar	whole-rock	14.1 ± 0.4	Duffield & McKee (1986)
SV31	–120.4140	41.2315	Tmvu	Pumice from tuff	$^{40}Ar/^{39}Ar$	plagioclase	14.09 ± 0.05	Carmichael et al. (2006)
D173B	–120.2200	41.4039	Tmba	Basalt	K-Ar	whole-rock	14.0 ± 0.4	Duffield & McKee (1986)
SV59	–120.4403	41.2295	Tmvu	Pumice from tuff	$^{40}Ar/^{39}Ar$	plagioclase	13.52 ± 0.06	Carmichael et al. (2006)
Middle Miocene Alturas Tuff								
SV136	–120.4148	41.2305	Tat	Basaltic andesite	$^{40}Ar/^{39}Ar$	groundmass	12.12 ± 0.05	Carmichael et al. (2006)
SV52-1	–120.5498	41.4593	Tat	Andesite glass	$^{40}Ar/^{39}Ar$	whole-rock	12.02 ± 0.06	Carmichael et al. (2006)
SV52-2	–120.5498	41.4593	Tat	Andesite glass	$^{40}Ar/^{39}Ar$	whole-rock	11.90 ± 0.08	Carmichael et al. (2006)
SV52-3	–120.5498	41.4593	Tat	Andesite glass	$^{40}Ar/^{39}Ar$	whole-rock	11.83 ± 0.10	Carmichael et al. (2006)
Late Miocene silicic rocks								
OH1	–120.3250	41.8500	Tmr	Obsidian	K-Ar	whole-rock	9.2 ± 0.3	Duffield & McKee (1986)
SH1	–120.3233	41.7967	Tmr	Obsidian	K-Ar	whole-rock	7.9 ± 0.2	Duffield & McKee (1986)
BC1	–120.2533	41.7081	Tmr	Obsidian	K-Ar	whole-rock	7.3 ± 0.3	Duffield & McKee (1986)
Late Miocene-Pliocene basalts								
SV154	–119.9985	41.6792	Tlb	Basaltic andesite	$^{40}Ar/^{39}Ar$	groundmass	8.08 ± 0.09	Carmichael et al. (2006)
SV161	–119.8750	41.8312	Tlb	Basalt	$^{40}Ar/^{39}Ar$	groundmass	8.03 ± 0.08	Carmichael et al. (2006)
SV6	–119.8547	41.8623	Tlb	Basalt	$^{40}Ar/^{39}Ar$	groundmass	7.69 ± 0.07	Carmichael et al. (2006)
SV24	–120.0745	41.8403	Tlb	Basaltic andesite	$^{40}Ar/^{39}Ar$	groundmass	7.33 ± 0.06	Carmichael et al. (2006)
SV134	–120.0505	41.6585	Tlb	Basalt	$^{40}Ar/^{39}Ar$	groundmass	5.95 ± 0.08	Carmichael et al. (2006)
SV13	–119.9582	41.9065	Tlb	Basalt	$^{40}Ar/^{39}Ar$	groundmass	4.91 ± 0.10	Carmichael et al. (2006)
SV35	–120.5028	41.2615	Tlb	Basalt	$^{40}Ar/^{39}Ar$	groundmass	4.61 ± 0.15	Carmichael et al. (2006)
SV132	–120.0468	41.5987	Tlb	Basalt	$^{40}Ar/^{39}Ar$	groundmass	4.36 ± 0.13	Carmichael et al. (2006)
SV150	–119.9603	41.6425	Tlb	Basalt	$^{40}Ar/^{39}Ar$	groundmass	4.33 ± 0.08	Carmichael et al. (2006)
SV92	–120.6320	41.5011	Tlb	Basalt	$^{40}Ar/^{39}Ar$	groundmass	4.31 ± 0.18	Carmichael et al. (2006)
SV4	–120.0307	41.5845	Tlb	Basalt	$^{40}Ar/^{39}Ar$	groundmass	4.28 ± 0.16	Carmichael et al. (2006)
SV27	–120.4400	41.4283	Tlb	Basalt	$^{40}Ar/^{39}Ar$	groundmass	3.98 ± 0.06	Carmichael et al. (2006)
SV18	–119.9843	41.5593	Tlb	Basalt	$^{40}Ar/^{39}Ar$	groundmass	3.84 ± 0.06	Carmichael et al. (2006)
SV162	–119.9615	41.9947	Tlb	Basalt	$^{40}Ar/^{39}Ar$	groundmass	3.81 ± 0.15	Carmichael et al. (2006)
SV137	–120.5157	41.3765	Tlb	Basalt	$^{40}Ar/^{39}Ar$	groundmass	2.94 ± 0.10	Carmichael et al. (2006)
SV139	–120.3263	41.3142	Tlb	Basalt	$^{40}Ar/^{39}Ar$	groundmass	2.76 ± 0.20	Carmichael et al. (2006)

*Precision of Lat/Long as originally reported. Locations in this study are NAD27 coordinates. Coordinate systems used by Carmichael et al. (2007) and Duffield & McKee (1986) are not specified and assumed to be NAD27. Coordinates for Axelrod (1966) given in township, section, range; lat/long were determined approximately.

†Precision of ages as originally reported. All $^{40}Ar/^{39}Ar$ dates calculated relative to Fish Canyon Tuff sanidine = 28.02 Ma.

§See references for complete source information.

#Corrected age—published age of 40.0 ± 3.0 used 4.72 x 10^{-30}/yr as the decay constant for K.

**We do not use these two ages in our determination of the age of the Cedar Pass complex, as the MSWD values are >100.

††Carmichael et al. (2006) refer to this unit as the Fortynine Tuff.

4.0 Ma (K-Ar) (Wells, 1980). The mineralogy and stratigraphy of these andesitic sequences suggest a subduction-related arc origin (Martz, 1970; Wells, 1980). Thus the latest Eocene in the Warner Range marks the return of arc magmatism to the general region after a hiatus of perhaps as much as 40 m.y. (represented by the time gap between the youngest intrusive rocks of the Sierra Nevada batholith ages of ca. 80 Ma and the earliest documented Tertiary andesitic lavas), although the predominance of debris flows and lahars over lava flows suggests these deposits were distal with respect to their volcanic sources.

Along the length of most of the Warner Range, a thick section of sedimentary and volcaniclastic rocks is exposed and was originally called the Lower Cedarville Formation by Russell (1928) (Plate 1). Based on detailed mapping in a portion of the range between Cedarville and Lake City (Fig. 3), Martz (1970) subdivided the Lower Cedarville Formation into three units; from oldest to youngest, these are the Steamboat Formation, the Deep Creek Formation, and the Lost Woods Formation (see Egger et al. [2009] for a complete discussion of formation names). The mapping presented here confirms the formation boundaries suggested by Martz (1970) and extends these subdivisions south of Cedar Pass (Fig. 3, Plate 1), where we use his formation names.

The Steamboat Formation (Tsbn, Tscc, and Tsu) is a cliff-forming, coarse-grained alluvial sandstone and conglomeratic sequence that ranges from ~1500 m thick in its southernmost exposures to 200 m thick where it is encountered in a drill core (Figs. 3 and 4) (Egger et al., 2009). In addition to this change in thickness, paleocurrent indicators and detrital zircon ages indicate a proximal volcanic source to the SSW, most likely within 20 km (Egger et al., 2009). Several dates on thin tuffs and reworked tuffs within the Steamboat Formation (Table 1) all suggest it was deposited between ca. 33 Ma and ca. 30 Ma (Duffield and McKee, 1986; Myers, 1998). Thin lake deposits contain abundant leaf fossils, and paleofloral analysis suggests paleoelevations of 1–2 km (Myers, 1998; Myers, 2003).

The Deep Creek Formation (Tdc) consists primarily of tuffs and reworked tuffaceous sediments, and generally forms a tree-covered slope above the conglomeratic cliffs of the Steamboat Formation. Martz (1970) described these tuffs as “welded,” but more often they are silicified and slightly hydrothermally altered to a greenish tint. Duffield and McKee (1986) dated an andesitic ash at 28.8 ± 1.1 Ma (K-Ar, hornblende) that may be from unit Tdc (Table 1).

The Lost Woods Formation (Tlw) consists of conspicuously red-weathering volcanic breccias, volcaniclastic sandstones and conglomerates, minor mafic tuff, and autobrecciated lava

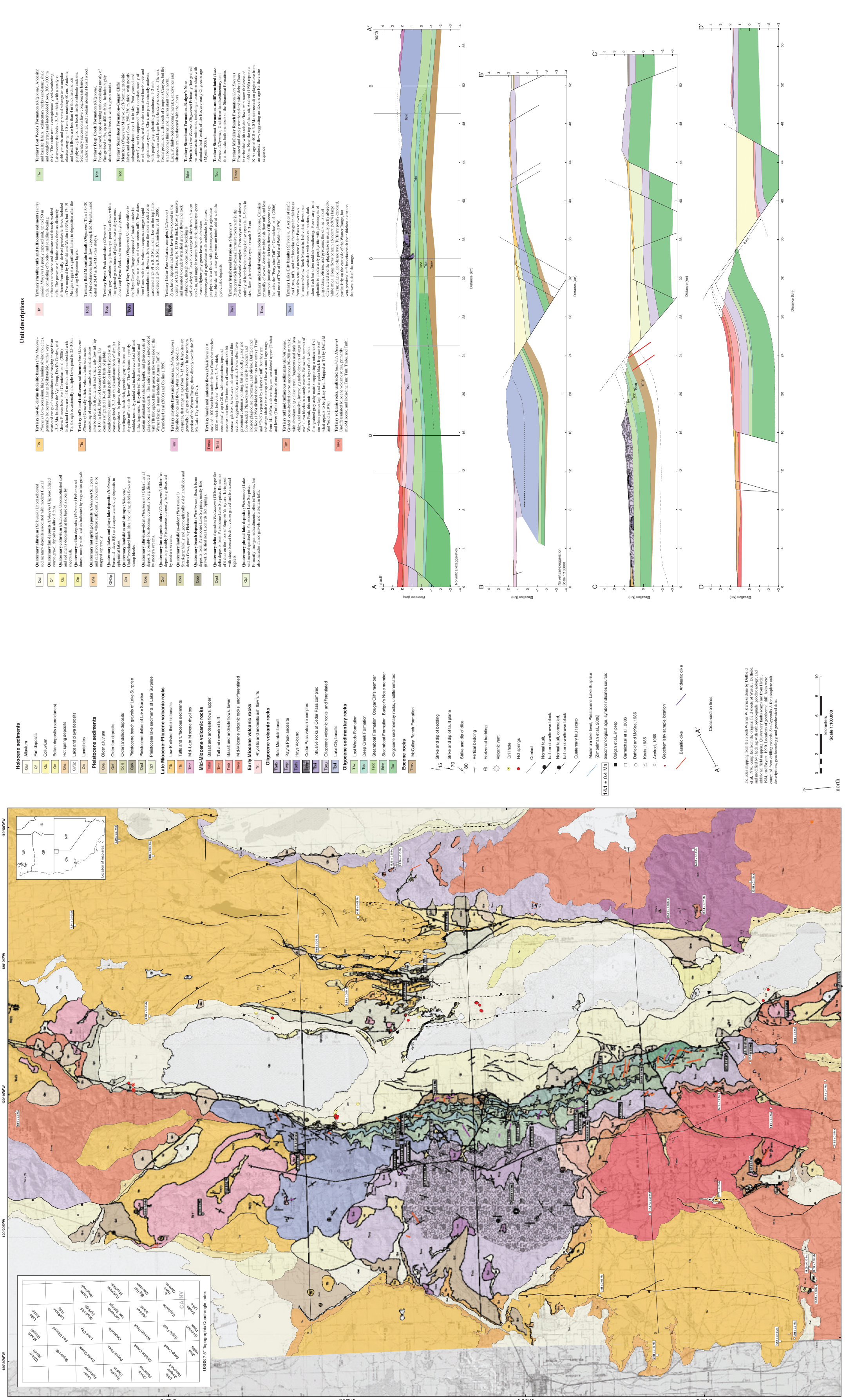

Plate 1. Geologic map and cross sections of the Warner Range and surrounding region at 1:100,000 scale. If you are viewing the PDF of this paper or reading it offline, please visit http://dx.doi.org/10.1130/GES00620.S1 or the full-text article on www.gsapubs.org to view the full-sized PDF file of Plate 1.

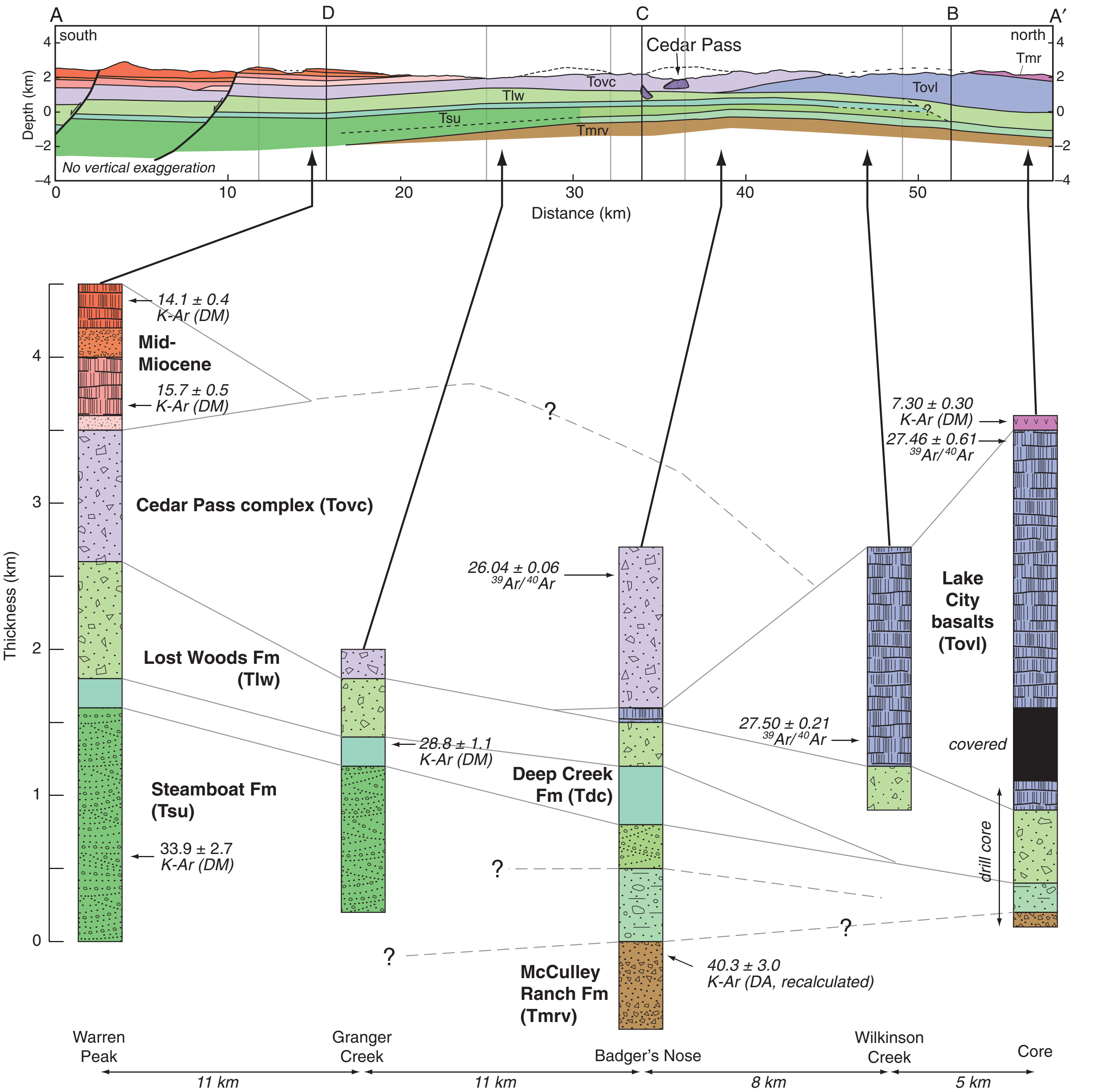

Figure 4. Stratigraphic columns of units exposed in the Warner Range and cross-section A–A′, showing likely correlations and age relationships of units. On cross section, gray lines correspond to bends in section (Plate 1); lettered black lines indicate crossing lines with perpendicular cross sections (Fig. 6). Selected geochronologic ages are from Duffield and McKee (1986)—DM, Axelrod (1966)—DA, and all others are from Colgan et al., 2010. FM—Formation.

flows. This unit contains more basalt than the underlying volcaniclastic sequence, and many of the breccias consist of homogeneous vesicular basalt clasts. In finer-grained sedimentary layers, Tlw includes petrified logs up to 1 m in diameter (Fig. 5A). On the ridge south of Cedar Pass, where the Lost Woods Formation is most extensively exposed, we measured orientations of the long axes of 13 of these logs (Fig. 5B), which are reliable indicators of paleofluvial transport direction (Fritz and Harrison, 1985). Though the number of samples is fewer than ideal, the nearly N-S trend of the majority of logs is apparent, indicating a roughly similar source direction as that of the underlying Steamboat Formation, though it is unclear, based on the logs alone, if the flow direction would have been to the north or the south. No units within

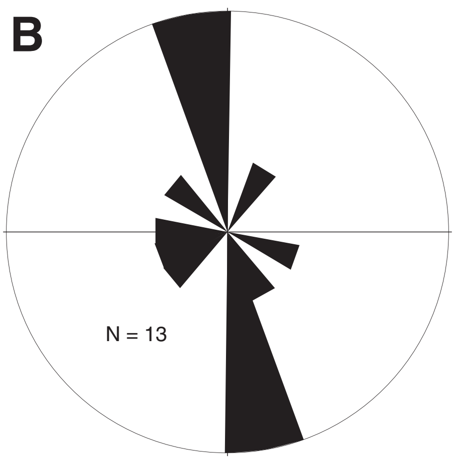

Figure 5. (A) Photograph of petrified logs in Lost Woods Formation. (B) Rose diagram showing orientation of petrified logs in Lost Woods Formation.

the Lost Woods Formation have been dated but its age is fairly well constrained between ca. 29 and 27.5 Ma based on ages from rocks in units above and below (Fig. 4).

This entire sequence of ca. 40–27.5 Ma volcaniclastic and sedimentary rocks was deposited in a continental basin within a system of active volcanoes—an intra-arc basin, as suggested by the presence of numerous ash layers, coarse volcanic breccias, highly variable thickness of units, and the presence of occasional lava flows throughout the sequence (Duffield and McKee, 1986; Egger et al., 2009; Martz, 1970). The spatial extent of this intra-arc basin is unknown, but a similar (although much thinner) sequence is exposed near Drake Peak (Fig. 2) ~100 km north of the study area (Wells, 1980), suggesting it could be at least 100 km long in its north-south dimension.

Oligocene (ca. 27.5–24 Ma) Arc Volcanic Rocks

Our mapping has indicated that the Warner Range and adjacent Hays Canyon Range to the east expose remnants of three late Oligocene volcanic edifices: the Lake City basalts (called the Soldier Creek volcanics by Martz [1970]), the Cedar Pass complex (our name), and the Hays Volcano (name given by Carmichael et al. [2006]). These three edifices and additional, more distal volcanic deposits (Tovu) are very closely related in space and time, as is typical of volcanic edifices within the modern Cascade arc (Hildreth, 2007). The geochemistry and geochronology of this Oligocene sequence is described in more detail by Colgan et al. (2011). Map relations and unit descriptions are summarized here.

The Lake City basalts (Tovl), a sequence of basalt and basaltic andesite flows and mafic tuffs, are exposed in the northern Warner Range where they reach a thickness of more than 2 km (Fig. 4). We have mapped this sequence thinning to the south, pinching out completely just north of Cedar Pass, indicating the flows likely represent part of a basaltic shield volcano (Fig. 4, Plate 1). The sequence ranges in age from 27.83 ± 0.21 Ma at the base of the sequence to 25.70 ± 0.94 Ma at the top (Table 1; Colgan et al., 2011). The cinder-rich mafic tuffs are thickest ~10 km north of Cedar Pass, suggesting a vent area in this general area (Figs. 3and 4, Plate 1). The Lake City basalts are similar in composition to the basaltic andesite of Twelvemile Peak, described by Wells (1980) and exposed ~80 km to the north; it is likely the two units are of similar age.

The Cedar Pass complex (Tovc) consists primarily of volcanic breccias, hornblende-rich andesite and basaltic andesite flows, and minor shallow dacite intrusions (Fig. 6). We have mapped a series of dikes of hornblende andesite that radiate out from a center ~5 km southwest of Cedar Pass in Dry Creek Basin (Plate 1). In addition, we mapped breccias that dip radially away from Dry Creek Basin, suggesting a vent location in this area (Plate 1, Fig. 3), a likelihood also noted by Duffield and McKee (1986). Numerous dates within the complex all fall within 26.6–27.0 Ma (Table 1; Colgan et al., 2011), suggesting the rapid development of an andesitic composite volcano or dome complex on the flank of the slightly older basaltic shield volcano (Tovl) to the north.

Farther south of the vent area, breccias disappear and contemporaneous Oligocene volcanics (Tovu) consist mostly of more distal andesite flows and ignimbrites (Plate 1) (Duffield and McKee, 1986). Duffield and Weldin (1976) mapped our Tovu as part of a "composite volcanic" unit, which they called Tvc. Geochronologic data (Table 1; Colgan et al., 2011) show that the Tvc unit of Duffield and Weldin (1976) contains a significant unconformity bracketed by the ca. 26–27 Ma Oligocene volcanic unit and the overlying early Miocene (ca. 19–17 Ma) welded tuffs, described below. We have therefore separated Duffield and Weldin's (1976) Tvc into two units: Tovu (Oligocene) and Trt (early Miocene) (Plate 1). Tovu is also exposed in the Hays Canyon Range to the east (Fig. 2, Plate 1). Carmichael et al. (2006) report an age of 26.26 ± 0.13 Ma on what they refer to as the Fortynine Tuff, which we include in Tovu (Plate 1). The Hays volcano (Tovh), exposed in the southern portion of the Hays Canyon Range, is a basaltic to basaltic andesite shield volcano dated at 23.8–24.5 Ma (Carmichael et al., 2006).

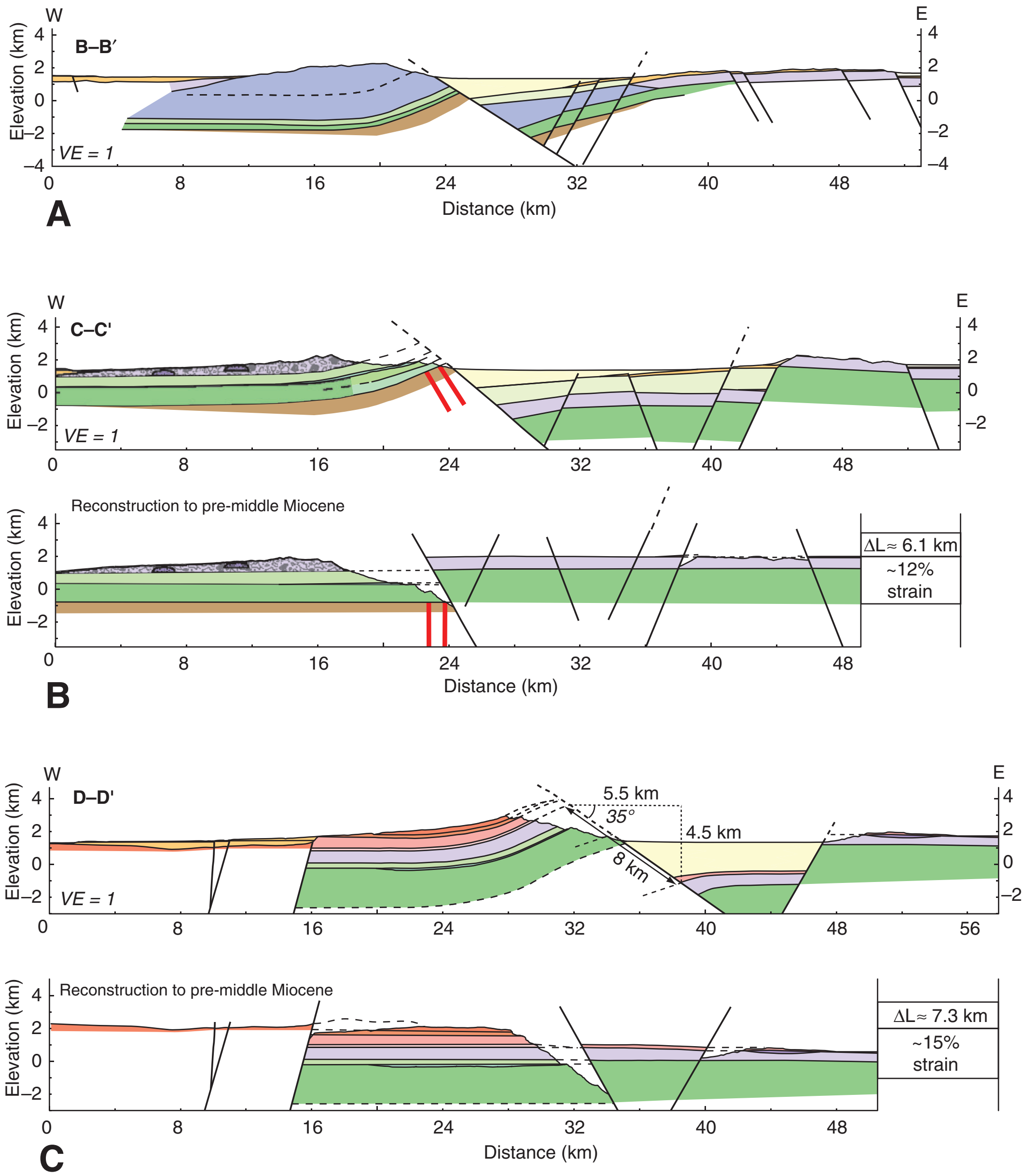

Figure 6. E-W cross sections, restored to preextensional configurations. Cross-section B–B′ is not restored because of the lack of units that can be tied across the fault. No vertical exaggeration (VE). See Figure 4 for color key and Plate 1 (and Fig. 3) for location of cross-section lines.

Major- and trace-element geochemistry of this sequence of 24–28 Ma volcanic rocks reveals that they are similar to rocks of both the modern and ancestral Cascade arc (Colgan et al., 2011). In contrast, coeval Oligocene volcanic rocks in the Black Rock Range and Pine Forest Range to the east (Fig. 2) comprise a bimodal sequence of basalt to basaltic trachyandesite and rhyolite tuffs (Colgan et al., 2006; Lerch et al., 2008). Although no rocks older than mid-Miocene are exposed on the Sheldon Plateau between the Warner and Black Rock Ranges, the volcanic edifices exposed in the Warner and Hays Canyon Ranges may mark the easternmost extent of subduction-related arc volcanism during the Eocene and Oligocene (e.g., Cousens et al., 2008).

Early Miocene Tuffs and Sediments

Few rocks of early Miocene age are preserved in the Warner Range, suggesting a near cessation of proximal volcanic activity ca. 24 Ma. A thin unit of rhyolitic tuffs and sediments (Trt) crops out between Parker Creek and Emerson Peak (Fig. 4, Plate 1), which Duffield and Weldin (1976) included in their unit Tvc. A new date of 19.22 ± 0.27 Ma on a reworked tuff at the base of this unit (Table 1; Colgan et al., 2011) suggests a 4–6 m.y. hiatus in deposition, followed by minor deposition of sediments and tuffs derived from distal, rhyolitic eruptions during the early Miocene, and thus we have separated this unit from Tvc of Duffield and Weldin (1976). Scarberry et al. (2010) report arc volcanic activity ca. 21–23 Ma in the Coleman Hills, near the Abert Rim in Oregon (Fig. 2), possibly representing the migration of arc volcanic activity north, away from the Warner Range region in the early Miocene.

Mid-Miocene Basaltic Volcanic Rocks

Despite the decrease in volcanic activity, it appears that relatively little erosion took place during this time, as Oligocene features still acted as topographic barriers to subsequent, younger volcanic flows and breccias. In the southern Warner Range, more than 1 km of basalts and basaltic andesites (Tmbl and Tmbu) and tuffs

(Tmt) were deposited from ca. 16 to 14 Ma (Table 1; Duffield and McKee, 1986), but our mapping indicates that these lavas were blocked from flowing north because of the topographic high formed by the Cedar Pass complex (Fig. 4, Plate 1). A similar relationship is observed in the Hays Canyon Range, where mid-Miocene basalt flows bank into the flanks of the Hays Volcano (Carmichael et al., 2006) (Plate 1), as well as farther north in Oregon (Fig. 2) (Scarberry et al., 2010; Wells, 1980).

The mid-Miocene age of these basalt flows initially led to their interpretation as part of the extensive Steens Basalt (e.g., Brueseke et al., 2007). However, the mid-Miocene volcanic rocks in the Warner and Hays Canyon ranges are geochemically distinct from the Steens basalt and instead are more similar to arc volcanic rocks of the Cascade Range (Colgan et al., 2011). In addition, the flows exposed in the Warner Range were erupted from mafic shield volcanoes such as those seen to the southwest of the Warner Range (Fig. 2), whereas the Steens basalts were erupted from a more diffuse network of dikes and form a flat-lying plateau (e.g., Camp et al., 2003).

Beginning ca. 15 Ma and continuing to ca. 7 Ma, the Warner Range and surrounding region experienced pulses of local rhyolitic magmatism (for locations mentioned below, see Figure 3), including the eruption of extensive ca. 15 Ma rhyolites south of Eagleville (Duffield and McKee, 1986), 12–14 Ma rhyolite magmatism coincident with gold mineralization in the High Grade District (Keats, 1985), and numerous rhyolite and obsidian domes erupted 7–9 Ma south of Fandango Pass, where they lie directly above Oligocene basalts (Fig. 4, Plate 1) (Duffield and McKee, 1986). These rhyolite domes mostly lie within the region of our reconnaissance mapping, and the ages and compositions are not known in detail.

Late Miocene to Pliocene Volcanic Rocks

Latest Miocene and Pliocene volcanic rocks in the region consist primarily of a distinctive series of low-potassium, high-alumina olivine tholeiites (Tlb) erupted between 8 and 3 Ma (Table 1); these rocks are described in detail elsewhere (Carmichael et al., 2006; McKee et al., 1983). These basalts are interbedded with rhyolite domes (Tmr) and tuffs and tuffaceous sediments (Tts). Geochemically, the compositions of the basalt flows show little variability (Figs. 6 and 7). Individual flows are thin, reaching only a few meters in thickness at most, but are interbedded with tuffs, tuffaceous sediments, and lacustrine deposits (Tts where mapped separately). The flows crop out extensively throughout the region, on both the west and east sides of the Warner Range and Surprise Valley fault (Plate 1). Despite their broad distribution, our mapping indicates that these flows were limited by preexisting topography of both the Hays Canyon and Warner ranges, in contrast to the interpretation of Carmichael et al. (2006) that they were once continuous across the southern Warner Range. On the east side of the Surprise Valley, a 3 Ma flow banks into the Oligocene tuffs of the Hays Canyon Range; on the west side, horizontal flows directly overlie Oligocene rocks west of the range (Plate 1). On the southwest side of the Warner Range, they appear to have flowed across preexisting normal faults, which may have also controlled the vent locations (Plate 1).

Our mapping shows that these flows were never, therefore, continuous across the region, and instead erupted simultaneously at several

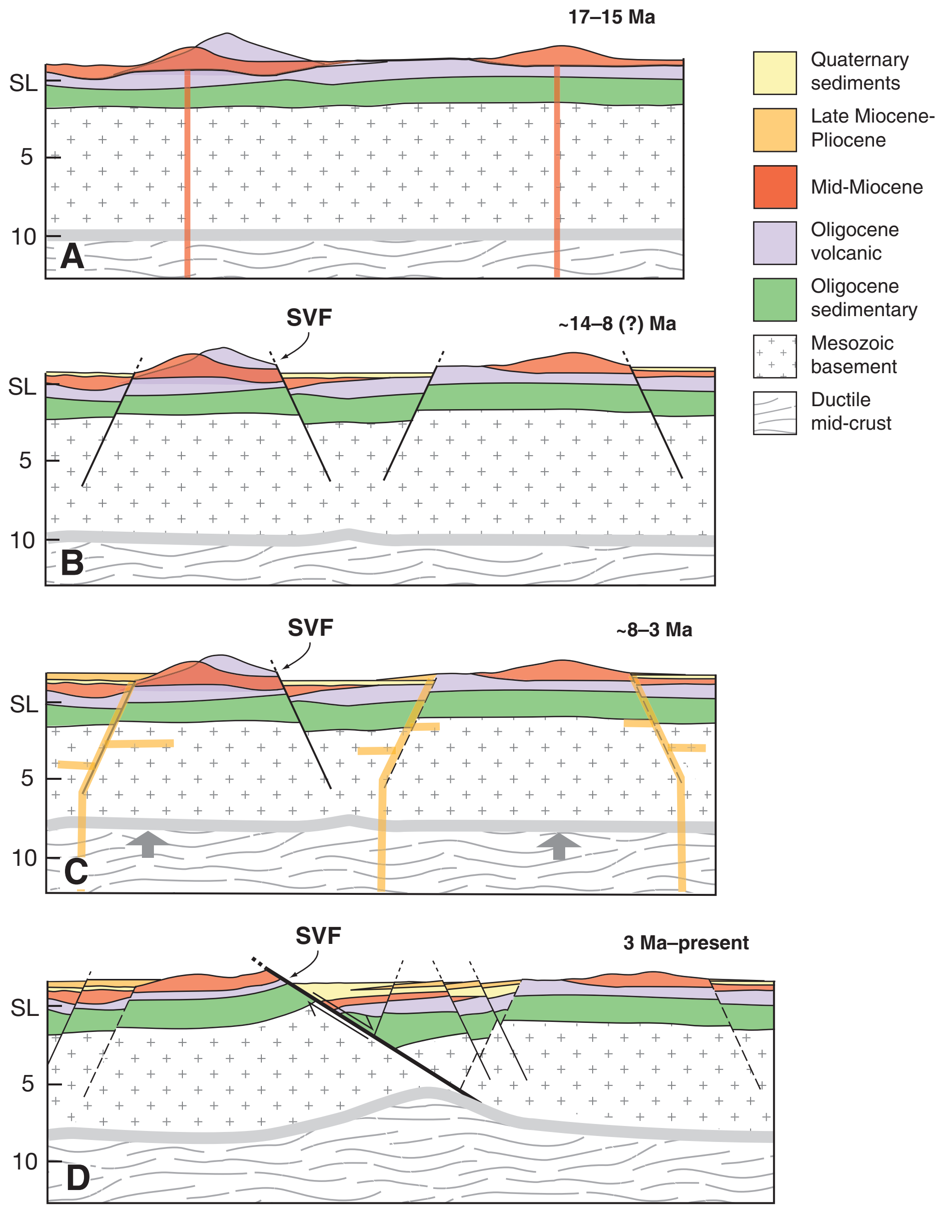

Figure 7. Schematic series of cross sections depicting the extensional history of the Warner Range region: (A) mid-Miocene volcanism, (B) onset of extension, (C) late Miocene–Pliocene volcanism, including dikes, which raises the brittle-ductile transition zone (gray line), and (D) Pliocene–present extension. Long dashed lines indicate faults that are no longer active. Thickness of line indicating fault represents relative offset—thicker lines indicate more offset.

locations, covering the low-lying areas with a thin veneer of basalt. Unlike the earlier Oligocene and Miocene volcanism, this magmatic event did not generate significant volcanic edifices, and what are likely volcanic vents appear as small, low-relief shields (Fig. 3) and plugs. Vents are located just north of the road between Vya and Cedarville, on the Devil's Garden Plateau, and on the west flank of the Warner Range (Fig. 3, Plate 1).

Pleistocene Lake Deposits

Pleistocene and younger deposits are dominated by sedimentary deposits from pluvial Lake Surprise, which reached a high stand of 1533.6 m (Zimbelman et al., 2008), filling the valley with water to a depth of ~156 m (~512 ft). Along the western side of the valley, the remains of several Gilbert-type fan deltas stand up to 30 m above the surrounding valley floor (Plate 1); our mapping provides additional detail where these were previously mapped (Duffield and Weldin, 1976) and adds newly mapped lake deposits in the northern basin. Numerous shorelines are visible, particularly at the southern end of the valley, where tufa deposits have cemented Pleistocene beach gravels (Zimbelman et al., 2008).

FAULTS AND EXTENSION

The rock units described above are cut and variably offset and tilted by a series of normal faults (Plate 1), which were mapped in greater detail in this study than in previous work. The most significant of these trend approximately north-south and include the range-bounding Surprise Valley and Hays Canyon faults (Fig. 3), of which the Surprise Valley fault has accommodated the most slip. Another set of faults and fractures trends NW-SE, paralleling a pervasive regional fracture system that becomes more prominent farther north in Oregon (Fig. 2). In the Warner Range region, the most significant NW-trending structure is the fault that forms Fandango Valley (Fig. 2, Plate 1). In the southern portion of the Warner Range, a set of four normal faults near Emerson Creek includes curved faults whose trends vary from NE-SW to N-S. These faults, referred to here as the Emerson Creek faults, are all down-to-the-E and -SE (the same sense as the Surprise Valley fault), accommodate up to several hundred meters of offset, and are covered by colluvium and cut by the Surprise Valley fault (Plate 1), indicating that they are no longer active. Finally, in the central portion of the Warner Range, we have mapped a previously unrecognized set of E-W–oriented normal faults that accommodate a few hundred meters of offset, at most, and appear to be entirely within the Oligocene sedimentary section (Plate 1). The remainder of this section deals primarily with the Surprise Valley and additional similarly oriented faults, which are most relevant for the discussion of extension in the region.

The majority of the uplift and tilt of units in the Warner Range is linked to motion along the Surprise Valley fault (SVF) (Fig. 3, Plate 1). The SVF includes several major segments connected by step-overs that primarily step to the left (Fig. 3), likely reflecting the growth and connection of a system of en echelon fault segments (e.g., Ferrill et al., 1999; Peacock, 2002). The most significant of these step-overs coincides with minor topographic highs in Surprise Valley, dividing the valley into a series of three subbasins that host the upper, middle, and lower lakes (Fig. 3, Plate 1). Numerous Quaternary fault scarps occur as far as 2 km from the main range-front fault (Fig. 3, Plate 1), cutting and displacing basin sediments by as much as 15 m (Hedel, 1980). The scarps are concentrated at the step-overs of the range-front fault, propagating into the basin (Fig. 3, Plate 1) and may be fault splays that initiate at the juncture of en echelon segment boundaries (e.g., Anders and Schlische, 1994).

A high-resolution seismic reflection profile reveals that the SVF now dips moderately (28° ± 6°) to the east (Lerch et al., 2010). The location of this profile (Fig. 3) is within one of the complex step-over zones along the range-bounding fault, and therefore the reflector imaged at this location may represent an anomalously shallow dip of the fault with respect to its average dip. Lerch et al. (2010) also model a 30°–40° east-dipping reflector at the latitude of Cedarville, which we believe to be more representative of the dip of the fault as a whole. Assuming a modern eastward dip of 35° (the average of 30°–40°) for the SVF and restoring the 25° of rotation for the most tilted units exposed in the range, the Surprise Valley fault may have initiated at an angle of ~60°, an angle that is well within the range expected for normal fault initiation (54°–69°) (e.g., Friedrich et al., 2004; Twiss and Moores, 1992). Based on the reasoning above, we assume a present-day angle for the SVF of 35° in cross section and utilize an initial 60° dip in restored cross sections (Fig. 6).

Roughly parallel to the SVF, a series of closely spaced normal faults cuts the late-Miocene to Pliocene volcanic rocks in the low hills north of the Hays Canyon Range (Fig. 3, Plate 1). The dip direction of these faults, as well as the amount of offset and tilt they accommodate, varies considerably along the length of the range, creating several tilt domains, shown schematically in Figure 3. On the eastern margin of the Upper Lake basin (Fig. 3), offset along east-dipping normal faults reaches several hundred meters, and fault-bound blocks are tilted and rotated up to 15° to the west (Fig. 6A, Plate 1). The faults die out and dips on the flows flatten to the north (Fig. 3, Plate 1). Within a given tilt domain, all basalt flows share similar dips, regardless of age, suggesting that faulting and tilting began after ca. 3 Ma.

These faults are most numerous and have the greatest offset just north of the road between Cedarville and Vya (Fig. 3, Plate 1), where several conjugate (west-dipping) faults have also developed, resulting in a series of interfingering horsts and grabens. This zone of more intense faulting likely represents a transverse antithetic accommodation zone (Fig. 3), as defined by Faulds and Varga (1998), which accommodates the transition from a half-graben in the upper lake basin (Fig. 6A) to a full graben in the middle and lower lake basins (Figs. 6B and 6C).

Utilizing the top of Tovu as a marker and the minimum depth to bedrock in Surprise Valley based on a drill hole log (Plate 1), we calculate a minimum of 8 km of dip-slip motion along the Surprise Valley fault near Warren Peak at cross-section D–D′, resulting in a stratigraphic throw of ~4.5 km (vertical component of dip-slip motion) and a horizontal component of slip of ~6.5 km as measured with respect to the present-day fault angle (Fig. 6C). Comparison of the distance between the eastern and western extents of cross-section D–D′ before and after restoration yields a total horizontal extension of 7.3 km across a distance of 50 km (~15% strain) since the mid-Miocene (Fig. 6C). A similar restoration of cross-section C–C′ yields a total horizontal extension of 6.1 km over ~51 km (~12% strain) across the same region since the mid-Miocene (Fig. 6B). The lack of units that can be tied across the fault further north precludes restoration of cross-section B–B′ (Fig. 6), but we assume that strain is 15% or less, given that the greatest strain is likely accumulated near the center of the fault.

DISCUSSION

Pre-Oligocene (40 Ma) Geologic Setting

No rocks older than ~40 Ma are exposed within ~100 km of the study area (Fig. 2), therefore little is known about the pre-late Eocene history of this region. The nearest exposures of pre-Tertiary rocks occur in the Black Rock Range, ~100 km to the east, where late Eocene (ca. 35 Ma) volcanic rocks were erupted across eroded Paleozoic metasedimentary rocks intruded by Cretaceous granite (Fig. 2) (Lerch et al., 2008). On the basis of seismic velocity and potential field modeling, Fuis et al. (1987) interpret plutonic basement (with a modeled $\rho = 2.73$ g/cm^3) to be shallow beneath the Warner Range—as little as 1 km below the exposed base of the section at Cedarville. Potential field modeling along a transect in Surprise Valley (Fig. 3) suggests that rocks of densities characteristic of continental basement (with a modeled $\rho = 2.67$ g/cm^3) are encountered ~1.5 km below the base of the rock sequence exposed in the Warner Range (Egger et al., 2010).

On the basis of apatite fission-track and (U-Th)/He dating of Cretaceous granites in northwestern Nevada, Colgan et al. (2006) concluded that 5 ± 2 km of material was eroded off the pre-Tertiary basement prior to deposition of Tertiary rocks, mostly during the late Cretaceous. By constructing an early Tertiary paleogeologic map from regional analysis of the basal Tertiary unconformity, Van Buer et al. (2009) inferred a similar history for the western Basin and Range and Sierra Nevada, where an erosional period lasting from ca. 85 to 45 Ma stripped as much as 5 km of material off the pre-Tertiary basement. We assume a similar history for basement rocks beneath the Warner Range region, such that, by the early Eocene, batholithic and/or metamorphic basement was exposed across a low-relief region of moderate elevation. This assumption is supported by the presence of granite cobbles in conglomerates near the base of the exposed section in the Warner Range (Duffield and Weldin, 1976; Egger et al., 2009). Based on these considerations, we show the depositional base of the stratified section of the Warner Range in cross section at a minimum depth of 0.5 km below the lowest exposed strata, and we infer that basement to be largely plutonic rocks of the Sierra Nevada batholith and the country rocks it intruded.

Magmatic History and Its Implications

From the late Eocene to the mid-Miocene, the Warner Range region was a site of arc volcanism, along with the western Cascades (du Bray et al., 2006). In the Oligocene (28–24 Ma) in particular, volcanoes within the active arc were located at the site of the modern Warner Range, where volcanic centers have the geomorphic expression of arc-related volcanoes, share geochemical features with contemporaneous volcanism in the western Cascades, and are in the geographic position behind the subduction zone at the time (see Colgan et al. [2011] for a detailed discussion of these relationships). Oligocene volcanic centers are also present near the modern Cascades, ~150 km to the west, indicating either that the arc was very wide at the time or that it has been subsequently extended. A velocity profile of the crust beneath the Modoc Plateau more closely resembles velocities seen beneath the Sierra Nevada than velocities in rifts such as the Salton Trough (Fuis et al., 1987), and thus significant extension in this area is unlikely. Modern volcanic arcs with widths >100 km are not common, but the Kurile-Kamchatka arc is one example (Volynets, 1994).

The arc volcanism that occurred in the Warner Range in the Oligocene was the result of subduction of the Juan de Fuca plate, distinguishing this northwestern corner of the Basin and Range from the rest of the province further east and south, which experienced magmatism that swept southward through time (Armstrong and Ward, 1991; Christiansen and Yeats, 1992). This regional pattern of magmatism is believed to have developed as the consequence of the peeling away of the shallow Laramide slab (Humphreys, 1995). Thus, the Warner Range region can be considered part of the "ancestral" Cascades. While the presence of an Oligocene ancestral arc farther south has been both supported (e.g., Busby et al., 2008; Cousens et al., 2008) and dismissed (e.g., Glazner and Farmer, 2008), the case is clearly in favor of an ancestral arc at the latitude of the Warner Range. In addition, subduction-related arc volcanism not only began here as early as in the western Cascades, but it continued sporadically in the Warner region through the mid-Miocene, becoming more mafic and generating smaller eruptive centers than during the earlier, Oligocene episode. This continued arc magmatism contrasts with the widespread flood basalts of similar age that blanketed the region further north and east (e.g., Hooper et al., 2002) (Fig. 1).

The Onset of Extension

Prior to the onset of extensional faulting in the mid-Miocene, therefore, the site of the modern Warner Range was characterized by significant topographic relief. The mid-Miocene volcanic edifices southwest of Eagleville (Fig. 2) rose as much as 500 m above the landscape, and the eroded remnants of the Oligocene volcanic centers rose at least some distance above the surrounding area. In fact, mid-Miocene relief is still locally present in this part of the Basin and Range; for instance, the mid-Miocene volcanic edifices south of the Warner Range are still barely eroded today (Fig. 2). Late Oligocene and early Miocene volcanic edifices produced long-lived topographic relief as evidenced by map relationships in both the Warner Range and farther north at Drake Peak (Wells, 1980) and near the Abert Rim in Oregon (Fig. 2) (Scarberry et al., 2010) where younger volcanic units have been shown to abut or thin toward older volcanic edifices.

In the southern portion of the Warner Range, the youngest rocks exposed at the crest are 14.1 ± 0.4 Ma (Duffield and McKee, 1986). Because the SVF and the Emerson Creek faults cut these rock units, the displacement associated with these faults must be younger than 14 Ma. It is not clear how much younger, however, and the geological constraints on their inception and timing of displacement are few. In the southern Warner and the Hays Canyon ranges, numerous 14–14.5 Ma basalt dikes that appear to be feeder dikes for the overlying mid-Miocene basalt flows trend N10°–35°W, averaging N25°W (Duffield and McKee, 1986). Several segments of the SVF roughly parallel the dike orientations (Plate 1), perhaps indicating that the fault initiated in the same stress regime and at about the same time. The Emerson Creek faults likely initiated at the same time, possibly acting as splay faults of the SVF near its southern termination (e.g., Anders and Schlische, 1994). The traces of these faults are now covered with thick colluvium, however, indicating that motion on these faults ceased and the SVF became the dominant fault. In the northern Warner Range, in contrast to the southern portion, rhyolite domes as young as 7.3 ± 0.3 Ma (Duffield and McKee, 1986) cap the range. Late Miocene volcanic rocks occur on both sides of the SVF at this latitude (Plate 1), but it has not proven possible to definitively tie a particular unit across the fault.

These geologic relationships suggest three possibilities for initiation of extensional faulting in the region: (1) motion along the entire Surprise Valley fault (and Emerson Creek faults) initiated at or shortly after 14 Ma and younger volcanic units in the northern part of the range were erupted at a later time on both sides of the SVF, (2) motion along the SVF initiated only after 7 Ma, or (3) motion along the SVF initiated in the south shortly after 14 Ma and migrated northward over the next 5–10 m.y., a phenomenon observed along the Abert Rim in Oregon (Scarberry et al., 2010). The existing thermochronology, though minimal, indicates that some exhumation or cooling may have occurred between 14 and 8 Ma, which suggests that the Surprise Valley fault initiated during that time frame and that (2) is therefore not likely. It is not possible to distinguish between (1) and (3) with existing mapping, geochronology, and thermochronology, but based on the presence of late Miocene rocks in the north (but not in the south), we suggest that motion along the SVF began in the south around 14 Ma and propagated northward, reaching the northern Warner Range after ca. 7 Ma.

Late Miocene to Pliocene Extension

By 4 Ma, there was enough relief generated by slip on both the Warner and Hays Canyon range-bounding faults that basalt flowing down the Surprise Valley banked unconformably into Oligocene and mid-Miocene volcanic rocks along the valley margins. On the western flank of the Warner Range, a basalt flow dated at 2.76 ± 0.20 Ma (Carmichael et al., 2006) covers a preexisting normal fault, which may have also controlled the vent location for these flows (Plate 1). These late Miocene and Pliocene basalt flows that range in age from ca. 8 to 3 Ma (Carmichael et al., 2006) are clearly cut by normal faults on both the west and east side of the Warner Range (Fig. 6, Plate 1), indicating a second episode of extension and uplift after the deposition of these units.

This younger episode of extension continues to the present, although the SVF has not been seismically active in historical times and even small earthquakes are relatively infrequent in this region compared with the rest of northern California (Uhrhammer, 1991) (Figs. 1 and 2). The potential for major (greater than magnitude 6) earthquakes is significant, however. A recent paleoseismology study of the Surprise Valley fault revealed evidence for five surface-rupturing earthquakes in the last 18 ka, the most recent of which occurred 1.2 ± 0.1 ka (Personius et al., 2009). A geodetic survey across the northern and western Basin and Range calculated an E-W extension rate of 1.6 ± 0.3 mm/yr across the SVF based on measurements of the differential horizontal velocity between two stations, one near the crest of the Warner Range (CEDR) and another on the east side of the valley (ALKA) (Fig. 3) (Hammond and Thatcher, 2007), although the authors have recently revised their estimate of extension rate down to 1.0 mm/yr (W. Thatcher, 2009, written commun.).

Colgan et al. (2008) proposed two phases of slip and exhumation along the Surprise Valley fault on the basis of thermochronometry of apatite from a single granite cobble from the base of the exposed sedimentary section in the Warner Range (see Figure 3 for sample location). Modeling of apatite fission track ages and track lengths in this sample suggest a poorly constrained phase of exhumation and cooling between ca. 14 and 8 Ma that may account for about one-third of the total exhumation of the sample. (U-Th)/He dating of apatites from the same sample suggests a period of rapid cooling and exhumation between ca. 3 Ma and 1 Ma that could account for most of the remaining two-thirds of the exhumation, though additional slip (on the order of 500–700 m, assuming a geothermal gradient of 35–40 °C) is required since 1 Ma to exhume the sample to its present exposure elevation (Colgan et al., 2008). The results of our work add evidence to the argument for two episodes of extension here.

As a result of extension and uplift since the mid-Miocene, rock units near the crest of the Warner Range inferred to be subhorizontal prior to slip on the Surprise Valley fault now dip as much as 20°–25° to the west and flatten to horizontal westward over a distance of ~10 km (Plate 1, Fig. 6C). Footwall flexure is an expected result of footwall unloading and isostatic compensation produced by motion along steeply dipping normal faults (Buck, 2007, and references therein; Thompson and Parsons, 2009). In the case of the Surprise Valley fault, the imaged Moho shows no evidence of rise or truncation related to the Surprise Valley fault at depth (Fig. 2) (Lerch et al., 2007). Because of the lack of Moho offset or pull-up, it is reasonable to conclude that the tilting and flexure seen in the upper crust are accommodated in the mid to lower crust by flow. Mid- and lower-crustal flow has been well documented in the Basin and Range, where the Moho remains flat despite variable upper crustal extension (Gans, 1987; Klemperer et al., 1986). Heat flow in the region, as measured in numerous wells (Raines et al., 1996), reaches 90–100 mW/m^2, higher even than the average for the Basin and Range (Blackwell et al., 1991). Surface heat flow of this magnitude suggests a geothermal gradient as high as 40–45 °C/km, and thus a local brittle-ductile transition zone (assumed to occur at 350 °C) at <8 km depth, facilitating the accommodation of flexure by flow in the mid-crust (e.g., Lerch et al., 2010).

Extensional Faulting History in the Context of Basin and Range Evolution

When extension began in the mid-Miocene, the Surprise Valley fault moved in isolation from other major Basin and Range faults, which currently lie nearly 100 km away in the extension direction across the Sheldon Plateau (Fig. 2). Why might extension have localized here, while the typical spacing of Basin and Range normal faults is closer to 20–30 km across the rest of the province (Stewart, 1971)? Temperature, composition, magmatism, and preexisting crustal weaknesses are all factors that can cause localization of extensional strain (e.g., Buck, 2007). One possibility is that Yellowstone hotspot volcanism, which began in the region 16–17 Ma (prior to extension), resulted in strengthening of the crust through the addition of mafic material to the lower crust, if boundary conditions that would allow extension were not present at that time. At most, however, hotspot activity only predates the onset of extension by ca. 5 Ma, which is insufficient time for crust that has been weakened by hotspot volcanism to cool and for the strength of mafic underplating to take effect. It is difficult to ignore, however, that the spatial distribution of the oldest Yellowstone-related calderas correlates geographically with the region currently lacking normal faults (Fig. 2) (Coble and Mahood, 2008), and this correlation may help explain the wider-than-average spacing of normal faults in this region. Regardless of the initiating mechanism, once the Surprise Valley fault was established, additional strain would have preferentially been accommodated along this existing structure, resulting in the accumulation of a minimum of 8 km of dip-slip—an amount comparable to some of the largest faults in the Basin and Range like the Schell Creek fault (Gans and Miller, 1983) and the White Mountain fault zone (Stockli et al., 2003).

The Warner Range and surrounding region (the extent of Fig. 3) has experienced only limited, 12%–15%, extension since the mid-Miocene. The sequence of events by which this may have occurred and their relationship to the region's magmatic history is represented schematically in Figure 7. Rejuvenated arc-related magmatism erupted from basaltic volcanoes in the middle Miocene, primarily 16–14 Ma (Fig. 7A), filling preexisting, erosional topography with up to 1 km of basalts, basaltic andesites, and mafic tuffs. Arc-related volcanism ceased and horst-and-graben-style normal faulting began sometime after 14 Ma, propagating northward after 7 Ma and resulting in a limited amount of extension, perhaps 3%–5% (~1/3 of the total extension to correlate with thermochronologic modeling that suggests that 1/3 of the exhumation occurred between ca. 14 and 8 Ma) (Fig. 7B). Mafic volcanism resumed ca. 8 Ma; these melts may have been channeled through fractures and crustal weaknesses, as they reached the surface from a hot, shallow aesthenospheric mantle source and show very little crustal contamination (Fig. 7C) (Carmichael et al., 2006; McKee et al., 1983). The addition of these melts to the base of the crust was likely accompanied by a temperature increase in the crust that would have raised the brittle-ductile transition zone (Fig. 7C). When extension began again ca. 3 Ma, renewed slip along the Surprise Valley fault resulted in footwall flexure that was accommodated by flow in the mid-crust (Fig. 7D). This second episode of extension and slip on the fault resulted in most of the uplift, tilting, and exhumation of the Warner Range.

A protracted or two-part history of extension, such as that seen in the Warner Range, has been noted elsewhere in the western Basin and Range. Faulting began ca. 12 Ma in the Black Rock Range (Lerch et al., 2008) and Pine Forest Range (Fig. 2) (Colgan et al., 2006), as well as in the Verdi-Boca basin near Reno (Fig. 1) (Henry and Perkins, 2001). Somewhat earlier extension is documented in the Shawave Range (Fig. 2), where apatite fission-track ages across the exhumed Shawave pluton suggest an episode of exhumation that lasted from 14.5 ± 1.4 Ma to 12.9 ± 0.7 Ma (Whitehill, 2009). The timing of earlier fault slip and extension in the Warner Range is not well constrained, but one possibility is that the Shawave and Warner ranges represented the western boundary of extension ca. 14 Ma. While extension subsequently migrated westward at the latitude of the Shawave Range—possibly due to the northwestward propagation of dextral shear in the Walker Lane (e.g., Faulds et al., 2005)—the boundary of significant extension at the latitude of the Warner Range has remained where it was in the Miocene.

The second phase of extension in the Warner Range, beginning ca. 3 Ma, appears to be a widespread phenomenon along the western margin of the Basin and Range, and possibly in the interior of the province as well. The 3 Ma extensional episode is coeval with rejuvenation of extension in the Carson Range (Surpless et al., 2002), Wassuk Range (Stockli et al., 2002), and the Verdi-Boca basin (Henry and Perkins, 2001; Mass et al., 2009) (Fig. 1). Extension may have continued to 3 Ma or less in the Black Rock Range (Lerch et al., 2008) and Pine Forest Range (Colgan et al., 2006) (see Figure 2 for locations), but is lesser in magnitude than the extension that has been documented along much of today's western boundary of the province. Mass et al. (2009) suggest that this young episode of extension may be a consequence of accelerated rollback of the Juan de Fuca slab, but the ranges affected by young faulting extend south beyond the projected southern limit of the Juan de Fuca plate at ca. 3 Ma (Fig. 1), thus suggesting a different driving mechanism.

On the basis of a geodetic survey (see Figure 3 for station locations), Hammond and Thatcher (2007) proposed that a component of right-lateral strike-slip should be accommodated across the Surprise Valley fault. The highly corrugated, arcuate shape of the SVF (Fig. 3) precludes its ability to accommodate significant strike-slip motion, however, and Personius et al. (2009) see no evidence (such as flower structures) of strike-slip motion in a trench along a recent fault scarp. If strike-slip motion is occurring within the Surprise Valley, it is more likely partitioned from the range-bounding dip-slip motion, possibly occurring along more steeply dipping faults within the valley (Egger et al., 2010) or along the diffuse, northwest-trending fracture systems that intersect the Warner Range and become more prominent to the north (Fig. 2). If, indeed, strike-slip motion is occurring within the Surprise Valley, it would nearly double the width of the proposed northern continuation of the Walker Lane, which includes the Honey Lake fault (Fig. 2), and which is much more narrowly constrained farther south (Fig. 1), but there is no evidence of dextral slip here.

CONCLUSIONS

The Warner Range and surrounding region provide key insight into the development of the northwestern margin of the Basin and Range. The long history of subduction-related arc volcanism recorded in the >4-km-thick succession of volcaniclastic sediments and volcanic rocks represents a unique exposure at this latitude and marks the easternmost extent of, and the return to, normal subduction following the Laramide flat-slab subduction of the early Tertiary. In addition, arc-related magmatism continued in the region into the mid-Miocene, despite the nearby impingement of the Yellowstone hotspot and voluminous eruptions of continental flood basalts that blanketed much of the surrounding region.

The extensional history of the Surprise Valley fault shares some similarities with other portions of the western margin of the Basin and Range, despite its unique tectonic setting. Crosscutting relationships seen in the Warner Range region suggest two episodes of extension—the first in the mid- to late-Miocene, the second starting after ca. 3 Ma—that appear to be widespread events, though the timing of these two events still needs to be better constrained. In contrast to much of the Basin and Range, however, the Surprise Valley fault has been isolated from other similar normal faults by 80–100 km in the direction of extension throughout its existence, perhaps due to its location immediately west of a series of hotspot-related silicic calderas.

Although the total amount of extension from the Modoc Plateau into north-central Nevada may be as little as 5% since the middle Miocene (e.g., Wells and Heller, 1988), the majority of that extension was accommodated along the Surprise Valley fault, resulting locally in ~15% extension. While this is relatively minor, the Warner Range and Surprise Valley fault appears to have persisted as the westernmost boundary of Basin and Range extension since its initiation in the mid- to late Miocene. In contrast, extension has stepped westward over the past 15 Ma further south (e.g., Surpless et al., 2002). Today, the Surprise Valley fault remains the actively deforming western boundary of the Basin and Range.

ACKNOWLEDGMENTS

We would like to thank Wendell Duffield for generously providing copies of his original field maps of the southern Warner Range. Numerous students participated in field mapping in the region as well, including Sarah Aarons, Noah Athens, Lee Chang, Brad Christensen, Matt Coble, Christina Contreras, Steve Davis, James Dudley, Katy Elsbury, Valentina Fontiveros, Julie Fosdick, Pablo Garcia del Real, Gwyneth Hughes, Julia James, Hari Mix, Ilana Lohr-Schmidt, Christina Muñoz, Patrick Ostrye, Emily Pope, Shauna Reidel-Bash, Annie Scofield, Silas Stafford, Tom Stilson, Ariel Strickland, Nick Van Buer, and Carly York. This paper has benefited from conversations with and reviews by Joe Colgan, Simon Klemperer, Gail Mahood, Marty Grove, and Trobe Grose. The work was funded by NSF Tectonics EAR 0809226 awarded to E. Miller and a grant from the Levorsen Fund in the School of Earth Sciences at Stanford University awarded to A. Egger. Additional field expenses were funded by the California Geological Survey through a contract with Trobe Grose.

REFERENCES CITED

Anders, M.H., and Schlische, R.W., 1994, Overlapping faults, intrabasin highs, and the growth of normal faults: The Journal of Geology, v. 102, p. 165–180, doi: 10.1086/629661.

Armstrong, R.L., and Ward, P.L., 1991, Evolving geographic patterns of Cenozoic magmatism in the North American Cordillera; the temporal and spatial association of magmatism and metamorphic core complexes: Journal of Geophysical Research, v. 96, p. 13,201–13,224, doi: 10.1029/91JB00412.

Atwater, T., and Stock, J., 1998, Pacific-North America plate tectonics of the Neogene southwestern United States; an update: International Geology Review, v. 40, p. 375–402, doi: 10.1080/00206819809465216.

Axelrod, D.I., 1966, Potassium-argon ages of some western Tertiary floras: American Journal of Science, v. 264, p. 497–506, doi: 10.2475/ajs.264.7.497.

Bennett, R.A., Wernicke, B., Niemi, N.A., Friedrich, A.M., and Davis, J.L., 2003, Contemporary strain rates in the northern Basin and Range province from GPS data: Tectonics, v. 22, p. 1008–1038, doi: 10.1029/2001TC001355.

Benoit, D., Moore, J., Goranson, C., and Blackwell, D.D., 2005, Core hole drilling and testing at the Lake City, California geothermal field: Geothermal Resources Council Transactions, v. 29, p. 203–208.

Blackwell, D.D., Steele, J.L., and Carter, L.S., 1991, Heat-flow patterns of the North American continent; a discussion of the geothermal map of North America, *in* Slemmons, D.B., Engdahl, E.R., Zoback, M.D., and Blackwell, D.D., eds., Neotectonics of North America, Volume 1: Decade of North American Geology: Boulder, Colorado, Geological Society of America, p. 423–436.

Brueseke, M.E., Heizler, M.T., Hart, W.K., and Mertzman, S.A., 2007, Distribution and geochronology of Oregon Plateau (U.S.A.) flood basalt volcanism: The Steens Basalt revisited: Journal of Volcanology and Geothermal Research, v. 161, p. 187–214, doi: 10.1016/j.jvolgeores.2006.12.004.

Bryant, W.A., 1990, Surprise Valley and related faults, Lassen and Modoc counties, *in* California Division of Mines and Geology Fault Evaluation Report, Volume 217, 17 p.

Buck, W.R., 2007, Dynamic processes in extensional and compressional settings: The dynamics of continental breakup and extension, *in* Schubert, G., ed., Treatise on Geophysics: Amsterdam, Elsevier, p. 335–376.

Busby, C.J., Hagan, J.C., Putirka, K., Pluhar, C.J., Gans, P.B., Wagner, D.L., Rood, D., DeOreo, S.B., and Skilling, I., 2008, The ancestral Cascades Arc; Cenozoic evolution of the central Sierra Nevada (California) and the birth of the new plate boundary, *in* Wright, J.E., and Shervais, J.W., eds., Ophiolites, arcs, and batholiths: A tribute to Cliff Hopson: Geological Society of America Special Paper 438, p. 331–378, doi: 10.1130/2008.2438(12).

Camp, V.E., Ross, M.E., and Hanson, W.E., 2003, Genesis of flood basalts and Basin and Range volcanic rocks from Steens Mountain to the Malheur River Gorge, Oregon: Geological Society of America Bulletin, v. 115, p. 105–128, doi: 10.1130/0016-7606(2003)115 <0105:GOFBAB>2.0.CO;2.

Carmichael, I.S.E., Lange, R.A., Hall, C.M., and Renne, P.R., 2006, Faulted and tilted Pliocene olivine-tholeiite lavas near Alturas, NE California, and their bearing on the uplift of the Warner Range: Geological Society of America Bulletin, v. 118, p. 1196–1211, doi: 10.1130/B25918.1.

Cashman, P.H., Trexler, J.H., Muntean, T.W., Faulds, J.E., Louie, J.N., and Oppliger, G.L., 2009, Neogene tectonic evolution of the Sierra Nevada-Basin and Range transition zone at the latitude of Carson City, Nevada, *in* Oldow, J.S., and Cashman, P.H., eds., Late Cenozoic structure and evolution of the Great Basin-Sierra Nevada transition: Geological Society of America Special Paper 447, p. 171–188, doi: 10.1130/2009.2447(10).

Christiansen, R.L., and Yeats, R.S., 1992, Post-Laramide geology of the U.S. Cordilleran region, *in* Burchfiel, B.C., Lipman, P.W., and Zoback, M.L., eds., The Cordilleran Orogen—Conterminous U.S., Volume G-3: Decade of North America Geology: Boulder, Colorado, Geological Society of America, p. 261–406.

Coble, M.A., and Mahood, G.A., 2008, New geologic evidence for additional 16.5–15.5 Ma silicic calderas in northwest Nevada related to initial impingement of the Yellowstone hotspot: IOP Conference Series: Earth and Environmental Science, v. 3, p. 012002.

Colgan, J.P., Dumitru, T.A., McWilliams, M., and Miller, E.L., 2006, Timing of Cenozoic volcanism and Basin and Range extension in northwestern Nevada: New constraints from the northern Pine Forest Range: Geological Society of America Bulletin, v. 118, p. 126–139, doi: 10.1130/B25681.1.

Colgan, J.P., Egger, A.E., John, D.A., Cousens, B., Fleck, R.J., and Henry, C.D., 2011, Oligocene and Miocene arc volcanism in northeastern California: Evidence for post-Eocene segmentation of the subducting Farallon plate: Geosphere, doi: 10.1130/GES00650.1 (in press).

Colgan, J.P., Shuster, D.L., and Reiners, P.W., 2008, Two-phase Neogene extension in the northwestern Basin and Range recorded in a single thermochronology sample: Geology, v. 36, p. 631–634, doi: 10.1130/G24897A.1.

Cousens, B., Prytulak, J., Henry, C., Alcazar, A., and Brownrigg, T., 2008, Geology, geochronology, and geochemistry of the Miocene-Pliocene Ancestral Cascades arc, northern Sierra Nevada, California and Nevada: The roles of the upper mantle, subducting slab, and the Sierra Nevada lithosphere: Geosphere, v. 4, p. 829–853, doi: 10.1130/GES00166.1.

du Bray, E.A., John, D.A., Putirka, K., and Cousens, B.L., 2009, Geochemical database for igneous rocks of the ancestral Cascades Arc; southern segment, California and Nevada: U. S. Geological Survey Data Series, v. DS-0439.

du Bray, E.A., John, D.A., Sherrod, D.R., Evarts, R.C., Conrey, R.M., and Lexa, J., 2006, Geochemical database for volcanic rocks of the western Cascades, Washington, Oregon, and California: U. S. Geological Survey Data Series, v. DS-0155, 49 p.

Duffield, W.A., and McKee, E.H., 1986, Geochronology, structure, and basin-range tectonism of the Warner Range, northeastern California: Geological Society of America Bulletin, v. 97, p. 142–146, doi: 10.1130/0016-7606(1986)97<142:GSABTO>2.0.CO;2.

Duffield, W.A., and Weldin, R.D., 1976, Mineral resources of the South Warner Wilderness, Modoc County, California: U. S. Geological Survey Bulletin, v. B1385, 31 p.

Egger, A.E., Colgan, J.P., and York, C., 2009, Provenance and palaeogeographic implications of Eocene-Oligocene sedimentary rocks in the northwestern Basin and Range: International Geology Review, v. 51, p. 900–919, doi: 10.1080/00206810902949829.

Egger, A.E., Glen, J.M.G., and Ponce, D.A., 2010, The northwestern margin of the Basin and Range province: Part 2: Structural setting of a developing basin from seismic and potential field data: Tectonophysics, v. 488, p. 150–161, doi: 10.1016/j.tecto.2009.05.029.

Faulds, J.E., Henry, C.D., Hinz, N.H., Hammond, W.C., Kreemer, C., and Blewitt, G., 2005, Kinematics of the northern Walker Lane: An incipient transform fault along the Pacific-North American plate boundary: Geology, v. 33, p. 505–508, doi: 10.1130/G21274.1.

Faulds, J.E., and Varga, R.J., 1998, The role of accommodation zones and transfer zones in the regional segmentation of extended terranes, *in* Faulds, J.E., and Varga, R.J., eds., Accommodation zones and transfer zones: The regional segmentation of the Basin and Range Province: Geological Society of America Special Paper 323, p. 1–45, doi: 10.1130/0-8137-2323-X.1

Ferrill, D.A., Stamatakos, J.A., and Sims, D., 1999, Normal fault corrugation: Implications for growth and seismicity of active normal faults: Journal of Structural Geology, v. 21, p. 1027–1038, doi: 10.1016/S0191-8141(99)00017-6.

Friedrich, A.M., Lee, J., Wernicke, B.P., and Sieh, K., 2004, Geologic context of geodetic data across a Basin and Range normal fault, Crescent Valley, Nevada: Tectonics, v. 23, 24 p., doi: 10.1029/2003TC001528.

Fritz, W.J., and Harrison, S., 1985, Transported trees from the 1982 Mount St. Helens sediment flows: Their use as paleocurrent indicators: Sedimentary Geology, v. 42, p. 49–64, doi: 10.1016/0037-0738(85)90073-9.

Fuis, G.S., Zucca, J.J., Mooney, W.D., and Milkereit, B., 1987, A geologic interpretation of seismic-refraction results in northeastern California: Geological Society of America Bulletin, v. 98, p. 53–65, doi: 10.1130/0016-7606(1987)98<53:AGIOSR>2.0.CO;2.

Gans, P.B., 1987, An open-system, two-layer crustal stretching model for the eastern Great Basin: Tectonics, v. 6, p. 1–12, doi: 10.1029/TC006i001p00001.

Gans, P.B., and Miller, E.L., 1983, Field trip 6; Style of mid-Tertiary extension in east-central Nevada: Special Studies—Utah Geological and Mineral Survey, v. 59, p. 107–160.

Gashawbeza, E.M., Klemperer, S.L., Wilson, C.K., and Miller, E.L., 2008, Nature of the crust beneath northwest Basin and Range province from teleseismic receiver function data: Journal of Geophysical Research, v. 113, p. 14, doi: 10.1029/2007JB005306.

Glazner, A.F., and Farmer, G.L., 2008, Ancestral Cascades = modern Cascades: Geological Society of America Abstracts with Programs, v. 40, p. 98.

Greene, R.C., 1984, Geologic appraisal of the Charles Sheldon Wilderness Study Area, Nevada and Oregon: U. S. Geological Survey Bulletin, p. 13–34.

Hammond, W.C., and Thatcher, W., 2004, Contemporary tectonic deformation of the Basin and Range Province, Western United States; 10 years of observation with the Global Positioning System: Journal of Geophysical Research, v. 109, p. 403–423, doi: 10.1029/2003JB002746.

Hammond, W.C., and Thatcher, W., 2005, Northwest Basin and Range tectonic deformation observed with the Global Positioning System, 1999–2003: Journal of Geophysical Research, v. 110, p. 405–416, doi: 10.1029/2005JB003678.

Hammond, W.C., and Thatcher, W., 2007, Crustal deformation across the Sierra Nevada, northern Walker Lane, Basin and Range transition, western United States measured with GPS, 2000–2004: Journal of Geophysical Research, v. 112, p. 26, doi: 10.1029/2006JB004625.

Hedel, C.W., 1980, Late Quaternary faulting in western Surprise Valley, Modoc County, California [Master's thesis]: San Jose, California, San Jose State University.

Hedel, C.W., 1981, Map showing geothermal resources of the Lake City-Surprise Valley known geothermal resource area, Modoc County, California: Miscellaneous Field Studies Map, v. MF-1299.

Hedel, C.W., 1984, Maps showing geomorphic and geologic evidence for late Quaternary displacement along the Surprise Valley and associated faults, Modoc County, California: Miscellaneous Field Studies Map, v. MF-1429.

Henry, C.D., Faulds, J.E., and dePolo, C.M., 2007, Geometry and timing of strike-slip and normal faults in the northern Walker Lane, northwestern Nevada and northeastern California; strain partitioning or sequential extensional and strike-slip deformation?, *in* Roeske, S.M., Till, A.B., Foster, D.A., and Sample, J.C., eds., Exhumation associated with continental strike-slip fault systems: Geological Society of America Special Paper 434, p. 59–79, doi: 10.1130/2007.2434(04).

Henry, C.D., and Perkins, M.E., 2001, Sierra Nevada-Basin and Range transition near Reno, Nevada: Two-stage development at 12 and 3 Ma: Geology, v. 29, p. 719–722, doi: 10.1130/0091-7613(2001)029<0719:SNBART>2.0.CO;2.

Hildreth, W., 2007, Quaternary magmatism in the Cascades; geologic perspectives: U. S. Geological Survey Professional Paper, v. P 1744, p. 125.

Hooper, P.R., Binger, G.B., and Lees, K.R., 2002, Ages of the Steens and Columbia River flood basalts and their relationship to extension-related calc-alkalic volcanism in eastern Oregon: Geological Society of America Bulletin, v. 114, p. 43–50, doi: 10.1130/0016-7606(2002)114<0043:AOTSAC>2.0.CO;2.

Humphreys, E.D., 1995, Post-Laramide removal of the Farallon slab, western United States: Geology, v. 23, p. 987–990, doi: 10.1130/0091-7613(1995)023<0987:PLROTF>2.3.CO;2.

Johnson, J.A., Hawkesworth, C.J., Hooper, P.R., and Ben Binger, G., 1998, Major- and trace-element analyses of Steens Basalt, southeastern Oregon: U. S. Geological Survey Open-File Report, v. OF 98–0482, 30 p.

Jordan, B.T., Grunder, A.L., Duncan, R.A., and Deino, A.L., 2004, Geochronology of age-progressive volcanism of the Oregon High Lava Plains: Implications for the plume interpretation of Yellowstone: Journal of Geophysical Research, v. 109, p. 19, doi: 10.1029/2003JB002776.

Keats, D.G., 1985, Geology and mineralization of the high Grade District, Modoc County, California [M.S. thesis]: Corvallis, Oregon, Oregon State University.

Klemperer, S.L., Hauge, T.A., Hauser, E.C., Oliver, J.E., and Potter, C.J., 1986, The Moho in the northern Basin and Range province, Nevada, along the COCORP 40° N seismic-reflection transect: Geological Society of America Bulletin, v. 97, p. 603–618, doi: 10.1130/0016-7606(1986)97<603:TMITNB>2.0.CO;2.

Lerch, D.W., Klemperer, S.L., Egger, A.E., Colgan, J.P., and Miller, E.L., 2010, The northwestern margin of the Basin-and-Range Province, part 1: Reflection profiling of the moderate-angle (~30°): Surprise Valley Fault: Tectonophysics, v. 488, p. 143–149, doi: 10.1016/j.tecto.2009.05.028.

Lerch, D.W., Klemperer, S.L., Glen, J.M.G., Ponce, D.A., Miller, E., and Colgan, J., 2007, Crustal structure of the northwestern Basin and Range Province and its transition to unextended volcanic plateaus: Geochemistry, Geophysics, Geosystems, v. 8, p. 1–21, doi: 10.1029/2006GC001429.

Lerch, D.W., Miller, E., McWilliams, M., and Colgan, J., 2008, Tectonic and magmatic evolution of the northwestern Basin and Range and its transition to unextended volcanic plateaus: Black Rock Range, Nevada: Geological Society of America Bulletin, v. 120, p. 300–311, doi: 10.1130/B26151.1.

MacGinitie, H.D., 1941, A middle Eocene flora from the central Sierra Nevada: Carnegie Institution of Washington Publication, 178 p.

Martz, P.W., 1970, The geology of a portion of the northern Warner mountains, Modoc County, California [M.S. thesis]: Davis, California, University of California.

Mass, K.B., Cashman, P.H., and Trexler, J.H., 2009, Stratigraphy and structure of the Neogene Boca Basin, northeastern California; implications for late Cenozoic tectonic evolution of the northern Sierra Nevada, *in* Oldow, J.S., and Cashman, P.H., eds., Late Cenozoic structure and evolution of the Great Basin-Sierra Nevada transition: Geological Society of America Special Paper 447, p. 147–170, doi: 10.1130/2009.2447(09).

McKee, E.H., Duffield, W.A., and Stern, R.J., 1983, Late Miocene and early Pliocene basaltic rocks and their implications for crustal structure, northeastern California and South-central Oregon: Geological Society of America Bulletin, v. 94, p. 292–304, doi: 10.1130/0016-7606(1983)94<292:LMAEPB>2.0.CO;2.

Myers, J.A., 1998, Paleovegetational heterogeneity and the record of Eocene-Oligocene climate change in the interior Pacific Northwest [Ph.D. thesis]: Santa Barbara, California, University of California.

Myers, J.A., 2003, Terrestrial Eocene-Oligocene vegetation and climate in the Pacific Northwest: New York, New York, Columbia University Press, p. 171–185.

Myers, J.A., 2006, The latest Eocene Badger's Nose flora of the Warner Mountains northeast California; the "in between" flora: PaleoBios, v. 26, p. 11–29.

Oldow, J.S., 2003, Active transtensional boundary zone between the western Great Basin and Sierra Nevada block, western U.S. Cordillera: Geology, v. 31, p. 1033–1036, doi: 10.1130/G19838.1.

Peacock, D.C.P., 2002, Propagation, interaction and linkage in normal fault systems: Earth-Science Reviews, v. 58, p. 121–142, doi: 10.1016/S0012-8252(01)00085-X.

Personius, S.F., Crone, A.J., Machette, M.N., Mahan, S.A., and Lidke, D.J., 2009, Moderate rates of late Quaternary slip along the northwestern margin of the Basin and Range Province, Surprise Valley fault, northeastern California: Journal of Geophysical Research, v. 114, 17 p., doi: 10.1029/2008jb006164.

Pierce, K.L., and Morgan, L.A., 1992, The track of the Yellowstone hot spot; volcanism, faulting, and uplift: Geological Society of America Memoir 179, p. 1–53.

Proffett, J.M., and Dilles, J.H., 1984, Geologic map of the Yerington District, Nevada, Volume 77: Reno, Nevada, Nevada Bureau of Mines and Geology.

Raines, G.L., Sawatsky, D.L., and Connors, K.A., 1996, Great Basin Geoscience Database, Volume DDS-41: U.S. Geological Survey.

Reed, J.C., Wheeler, J.O., and Tucholke, B.E., 2005, Geologic Map of North America, Continent-Scale Map-001: Boulder, Colorado, Geological Society of America.

Russell, R.J., 1928, Basin Range structure and stratigraphy of the Warner Range, northeastern California: University of California Publications in Geological Sciences, v. 17, p. 387–496.

Scarberry, K.C., Meigs, A.J., and Grunder, A.L., 2010, Faulting in a propagating continental rift: Insight from the late Miocene structural development of the Abert Rim fault, southern Oregon, USA: Tectonophysics, v. 488, p. 71–86, doi: 10.1016/j.tecto.2009.09.025.

Stewart, J.H., 1971, Basin and Range structure: A system of horsts and grabens produced by deep-seated extension: Geological Society of America Bulletin, v. 82, p. 1019–1044, doi: 10.1130/0016-7606(1971)82[1019:BARSAS]2.0.CO;2.

Stockli, D.F., Dumitru, T.A., McWilliams, M.O., and Farley, K.A., 2003, Cenozoic tectonic evolution of the White Mountains, California and Nevada: Geological Society of America Bulletin, v. 115, p. 788–816, doi: 10.1130/0016-7606(2003)115<0788:CTEOTW>2.0.CO;2.

Stockli, D.F., Surpless, B.E., Dumitru, T.A., and Farley, K.A., 2002, Thermochronological constraints on the timing and magnitude of Miocene and Pliocene extension in the central Wassuk Range, western Nevada: Tectonics, v. 21, p. 10–28, doi: 10.1029/2001TC001295.

Surpless, B., 2008, Modern strain localization in the central Walker Lane, Western United States; implications for the evolution of intraplate deformation in transtensional settings: Tectonophysics, v. 457, p. 239–253, doi: 10.1016/j.tecto.2008.07.001.

Surpless, B., Stockli, D.F., Dumitru, T.A., and Miller, E.L., 2002, Two-phase westward encroachment of Basin and Range extension into the northern Sierra Nevada: Tectonics, v. 21, p. 1002–1014, doi: 10.1029/2000TC001257.

Thatcher, W., Foulger, G.R., Julian, B.R., Svarc, J., Quilty, E., and Bawden, G.W., 1999, Present-day deformation across the Basin and Range Province, Western United States: Science, v. 283, p. 1714–1718, doi: 10.1126/science.283.5408.1714.

Thompson, G.A., and Parsons, T., 2009, Can footwall unloading explain late Cenozoic uplift of the Sierra Nevada crest?: International Geology Review, v. 51, p. 986–993, doi: 10.1080/00206810903059156.

Trexler, J.H., Jr., Cashman, P.H., Henry, C.D., Muntean, T., Schwartz, K., Tenbrink, A., Faulds, J.E., Perkins, M., and Kelly, T., 2000, Neogene basins in western Nevada document the tectonic history of the Sierra Nevada–Basin and Range transition zone for the last 12 Ma, *in* Lageson, D.R., Peters, S.G., and Lahren, M.M., eds., Great Basin and Sierra Nevada: Boulder, Colorado, Geological Society of America Field Guide 2, p. 97–116.

Twiss, R.J., and Moores, E.M., 1992, Structural geology: New York, New York, W.H. Freeman and Company, 532 p.

Uhrhammer, R.A., 1991, Northern California seismicity, *in* Slemmons, D.B., Engdahl, E.R., Zoback, M.D., and Blackwell, D.D., eds., Neotectonics of North America, Volume 1: Decade of North American Geology: Boulder, Colorado, Geological Society of America, p. 99–106.

Unruh, J., Humphrey, J., and Barron, A., 2003, Transtensional model for the Sierra Nevada frontal fault system, eastern California: Geology, v. 31, p. 327–330, doi: 10.1130/0091-7613(2003)031<0327:TMFTSN>2.0.CO;2.

Van Buer, N.J., Miller, E.L., and Dumitru, T.A., 2009, Early Tertiary paleogeologic map of the northern Sierra Nevada batholith and the northwestern Basin and Range: Geology, v. 37, p. 371–374, doi: 10.1130/G25448A.1.

Volynets, O.N., 1994, Geochemical types, petrology, and genesis of late Cenozoic volcanic rocks from the Kurile-Kamchatka island-arc system: International Geology Review, v. 36, p. 373–405, doi: 10.1080/00206819409465467.

Wells, R.E., 1980, Drake Peak; a structurally complex rhyolite center in southeastern Oregon: U. S. Geological Survey Professional Paper, v. 1124-E, p. E1–E16.

Wells, R.E., and Heller, P.L., 1988, The relative contribution of accretion, shear, and extension to Cenozoic tectonic rotation in the Pacific Northwest: Geological Society of America Bulletin, v. 100, p. 325–338, doi: 10.1130/0016-7606(1988)100<0325:TRCOAS>2.3.CO;2.

Wesnousky, S.G., 2005, Active faulting in the Walker Lane: Tectonics, v. 24, 35 p., doi: 10.1029/2004TC001645.

Whitehill, C., 2009, Cenozoic evolution of the Shawave-Nightingale horst block, Northwestern Basin and Range, Nevada, U.S.A. [Ph.D. thesis]: Stanford, California, Stanford University.

Zimbelman, J.R., Garry, B., and Irwin, R.P., 2008, Field investigation of pluvial features in Surprise Valley as analogs for pluvial landforms on Mars: Geological Society of America Abstracts with Programs, v. 40, p. 294.

Manuscript Received 31 May 2010
Revised Manuscript Received 17 February 2011
Manuscript Accepted 21 February 2011